Drug Metabolism and Disposition

Manuscript # DMD-AR-2022-000957

Supplementary Material

Isolation and Identification of 3,4-Seco-Solanidine-3,4-dioic acid (SSDA) as a Urinary Biomarker of Cytochrome P450 2D6 (CYP2D6) Activity

Andrew C Behrle[1], Justin Douglas, J. Steven Leeder and Leon van Haandel[2]

Division of Clinical Pharmacology, Toxicology and Therapeutic Innovation, Department of Pediatrics, and Children's Mercy Research Institute, Children's Mercy Kansas City, Kansas City MO 64108, USA (A.C.B., J.S.L., L.vH.); Department of Chemistry, University of Kansas, Lawrence, KS 66045, USA (J.D.), and Schools of Medicine and Pharmacy, University of Missouri-Kansas City, Kansas City, MO, 64108, USA (J.S.L.)

Supporting Information Table of Contents

Supplemental Methods

Supplemental Results

Equation S1. Number of double bond equivalents.

Supplemental Figure S1. Enhanced view of ^{1}H NMR spectrum of solanidine showing four methyl resonances in CD_3OD. Insert showing C6-H (δ = 5.45, $^{3}J_{H\text{-}H}$ = 5.6 Hz, 1H) and C3-H (δ = 3.40, m, 1H) resonances.

Supplemental Figure S2. ^{1}H spectrum of SSDA

Supplemental Figure S3. Enhanced view of ^{1}H NMR spectrum of the unknown CYP2D6 biomarker showing four methyl resonances in CD_3OD. Insert showing methylylidene resonance.

Supplemental Figure S4. Stepwise connectivity model of unknown CYP2D6 biomarker. a = Ambiguous assignment of C-1, C-2 and C-24. X = C or heteroatom. Hydrogen atoms omitted for clarity.

Supplemental Figure S5. Stepwise connectivity model of unknown CYP2D6 biomarker. a = Ambiguous assignment of carbons 1, 2, 24. X = C or heteroatom. Hydrogen atoms omitted for clarity.

Supplemental Figure S6. 2D TOCSY with enhanced view of C2-H' correlations with C1-H' and/or C15-H'. Red circle represents missing C15-H correlation.

Supplemental Figure S7. 2D TOCSY with enhanced view of C1-H' and C1-H correlations C2-H' and C2-H.

Supplemental Figure S8. Stepwise connectivity model of unknown CYP2D6 biomarker. X = C or heteroatom. Hydrogen atoms omitted for clarity.

Supplemental Figure S9. Stepwise connectivity model of unknown CYP2D6 biomarker. X = C or heteroatom. Hydrogen atoms omitted for clarity.

Supplemental Figure S10. Stepwise connectivity model of unknown CYP2D6 biomarker. X = C or heteroatom; R = C or heteroatom; R' = C or heteroatom. Hydrogen atoms omitted for clarity.

Supplemental Figure S11. Stepwise connectivity model of unknown CYP2D6 biomarker. X = heteroatom. Hydrogen atoms omitted for clarity.

Supplemental Figure S12. $^{13}C\{^{1}H\}$ NMR spectrum of SSDA.

Supplemental Figure S13. Enhanced $^{13}C\{^{1}H\}$ NMR spectrum of SSDA.

Supplemental Figure S14. DEPT135 $^{13}C\{^{1}H\}$ NMR spectrum of SSDA.

Supplemental Figure S15. DEPT90 $^{13}C\{^{1}H\}$ NMR spectrum of SSDA.

Supplemental Figure S16. HSQC full spectrum of SSDA in CD_3OD.

Supplemental Figure S17. HSQC enhanced spectrum of SSDA in CD_3OD.

Supplemental Figure S18. HMBC spectrum of SSDA in CD_3OD.

Supplemental Figure S19. HMBC spectrum of SSDA in CD_3OD with C6−H correlations.

Supplemental Figure S20. HMBC enhanced spectrum of SSDA in CD_3OD.

Supplemental Figure S21. HMBC enhanced spectrum of SSDA in CD_3OD with C18−H, C19−H, C21−H and C27−H correlations.

Supplemental Figure S22. HMBC spectrum of SSDA in CD_3OD with long range J filter width = 6 Hz.

Supplemental Figure S23. HMBC enhanced spectrum of SSDA in CD_3OD with long range J filter width = 6 Hz.

Supplemental Figure S24. HMBC spectrum of SSDA in CD_3OD with long range J filter width = 4 Hz.

Supplemental Figure S25. HMBC enhanced spectrum of SSDA in CD_3OD with long range J filter width = 4 Hz.

Supplemental Figure S26. COSY spectrum of SSDA in CD_3OD.

Supplemental Figure S27. COSY enhanced spectrum of SSDA in CD_3OD with C6−H correlations.

Supplemental Figure S28. COSY enhanced spectrum of SSDA in CD_3OD.

Supplemental Figure S29. TOCSY spectrum of SSDA in CD_3OD.

Supplemental Figure S30. TOCSY enhanced spectrum of SSDA in CD_3OD with C6−H correlations.

Supplemental Figure S31. TOCSY enhanced spectrum of SSDA in CD_3OD.

Supplemental Figure S32. TOCSY enhanced spectrum of SSDA with view of C15-H correlations. Red circle represents missing correlation.

Supplemental Figure S33. HSQC−TOCSY enhanced spectrum of SSDA in CD_3OD.

Supplemental Figure S34. HSQC−TOCSY enhanced spectrum of SSDA in CD_3OD with C6−H correlations.

Supplemental Figure S35. HSQC−TOCSY enhanced spectrum of SSDA in CD_3OD.

Supplemental Figure S36. HSQC−TOCSY enhanced spectrum of SSDA in CD_3OD with spectral window.

Supplemental Figure S37. HSQC−TOCSY enhanced spectrum of SSDA in CD_3OD with C21−H and C27−H correlations.

Supplemental Figure S38. Amidation of SSDA with EDC and ethanolamine and chromatogram of first amidation product of SSDA.

Supplemental Figure S39. Chromatogram of second amidation product of SSDA.

Supplemental Table S1. qNMR Results

Supplemental Table S2. qNMR Results and step-by-step Workflow 100% Method to Determine Purity

Supplemental Table S3. qNMR Results and step-by-step Workflow IC Method to Determine Purity

Supplementary Methods

Description of chromatographic steps utilized for isolation and purification of M1

Initial Omnifit 10 cm C18 flash silica column purification. A 10 cm Omnifit chromatography column was charged with spherical C18 flash silica (45-75 μm, 70 Å) and activated with methanol on an Aligent 1100 series LC system at a flow rate of 5.0 mL/min for 30 minutes. The column was then equilibrated with a 95:5 H_2O/MeOH solution at a flow rate of 5.0 mL/min for 30 minutes. 500 mL of urine was loaded onto the column at a flow rate of 5.0 mL/min. The column was washed with 50 mL of H_2O. The column was eluted using a 50:50 H_2O/MeOH with 0.1% NEt_3, pH = 4.40 (adjusted using acetic acid) solution at a flow rate of 5.0 mL/min. 10 mL fractions were collected and a total of 12 fractions were collected. Fractions from each gallon were collected and kept separate from other gallons. The desired fractions were collected, combined, evaporated to dryness and the residue dissolved with 50 mL of 50:50 MeOH/10 mM NaOAc buffer, pH = 5.0.

LC-SCX-SPE purification. A 3 mL Supelclean LC-SCX SPE cartridge was attached to a vacuum manifold, activated with MeOH (6 mL) and equilibrated with 50 mM NaOAc buffer, pH = 5.0 (6 mL). The sample solution (10 mL of 50:50 MeOH/10 mM NaOAc buffer, pH = 5.0) was diluted to final volume of 100 mL using a water with 0.1% formic acid. The cartridge was charged with 10 mL of sample solution at a time (total of ten loadings) and each loading was collected in a separate 13x100 mm culture tube. The cartridge was charged with a 1.6% formic acid water solution v/v (6 mL) and the fraction was collected into a culture tube. The cartridge was charged with 80:20 50 mM NaOAc buffer, pH = 5.0/MeOH solution (8 mL, x3) and each fraction was collected in a separate culture tube. The M1 biomarker was eluted from the cartridge using a 50:50 MeOH/NH_4OH, 2-3% NH_3 solution (6 mL) and collected in a culture tube. All collected fractions were evaporated and dissolved with 10 mL of 90:10 10 mM NH_4OAc buffer, pH = 7.0/MeOH and analyzed. The desired fractions from each gallon were collected, combined, evaporated to dryness and the residue dissolved with 15 mL of 90:10 10 mM NH_4OAc buffer, pH = 7.0/MeOH solution.

Second Omnifit 10 cm C18 flash silica column purification. A 10 cm Omnifit chromatography column was charged with spherical C18 flash silica (45-75 μm, 70 Å) and activated with methanol solution containing 0.1% triethylamine and 0.1% acetic acid on an Aligent 1100 series LC system at a flow rate of 5.0 mL/min for 20 minutes. The column was then equilibrated with a 95:5 H_2O/MeOH (0.1% trimethylamine and 0.1% acetic acid) solution at a flow rate of 5.0 mL/min for 20 minutes. The sample was loaded onto the column 5 mL at a time (total of three columns used for each gallon). 25 mL fractions were collected and a total of 11 fractions were collected. Elution conditions for fractions 1-2 were 95:5 H_2O/MeOH (0.1% triethylamine and 0.1% acetic acid); elution conditions for fractions 3-4 were 80:20 H_2O/MeOH (0.1% triethylamine and 0.1% acetic acid); elution conditions for fractions 5-7 were 60:40 H_2O/MeOH (0.1% trimethylamine and 0.1% acetic acid); elution conditions for fractions 8-11 were 45:55 H_2O/MeOH (0.1% triethylamine and 0.1% acetic acid). The desired fractions from each gallon were collected, combined, evaporated to dryness and the residue was dissolved with 15 mL of 90:10 10 mM NH_4OAc buffer, pH = 7.0/MeOH solution.

C18 Sunfire Column purification. A syringe loading injector (Rheodyne model 7125) was attached to an I-Class Acquity UPLC with a flow-through needle (FTN) sample manager. A Waters C18 Sunfire column (5.0 μm, 4.6 x 150 mm) equipped with a Waters Sunfire C18 VanGuard Precolumn (5.0 μm, 3.9 x 5 mm) was connected to the syringe loading injector. Two 500 μL manual injections of the M1 biomarker solution were loaded onto the head of the column (two volume equivalents of sample loop), column was disconnected from syringe loading injector, connected to sampled manager and equilibrated. The following gradient was used on

the UPLC system: initial conditions of 1% B, ramping up linearly to 99% B at 10 minutes and held for 2 minutes. At 12.10, the column was stepped down to initial conditions. Mobile phases A and B were H_2O and MeOH both containing 0.1% formic acid, respectively. The flow rate was 0.7 mL/min and column temperature was set to 25 ˚C. Fractions at 0-6, 6-6:20, 6:20-6:40, 6:40-7, 7-7:20, 7:20-7:40, 7:40-8, and 8-13 minutes were collected and analyzed. The desired fractions from each gallon were collected, combined, evaporated to dryness and the residue was dissolved with 3 mL of 90:10 10 mM NH_4OAc buffer, pH = 7.0/MeOH solution.

Acquity UPLC BEH C18 Purification. A syringe loading injector (Rheodyne model 7125) was attached to an I-Class Acquity UPLC with a flow-through needle (FTN) sample manager. A Waters Acquity UPLC BEH C18 column (1.7 μm, 2.1 x 100 mm) equipped with a Waters Acquity UPLC C18 VanGuard Precolumn (1.7 μm, 2.1 x 5 mm) was connected to the syringe loading injector. 250 μL manual injection of the M1 biomarker solution was loaded onto the head of the column (two volume equivalents of sample loop), column was disconnected from syringe loading injector, connected to sampled manager and equilibrated. The following gradient was used on the UPLC system: initial conditions of 1% B, ramping up linearly to 99% B at 5 minutes and held for 3 minutes. At 8 minutes, the column was stepped down to initial conditions. Mobile phases A and B were 90:10 10 mM $(NH_4)(HCO_3)$ buffer, pH = 10/MeOH and MeOH (100%), respectively. The flow rate was 0.2 mL/min and column temperature was set to 25 ˚C. Fractions at 0-4:40, 4:40-5, 5-5:20, 5:40-6, 6-6:20, 6:20-6:40, 6:40-7, and 7-10 minutes were collected and analyzed. The desired fractions were collected, combined, evaporated to dryness and the residue dissolved with 1 mL of 50:50 MeOH/H_2O solution.

Xevo G2−XS QToF mass spectrometer settings. The Xevo G2-XS QToF mass spectrometer was operated in ESI+ mode. Analytes were separated on a Waters Acquity UPLC M-class trap symmetry C18 reversed-phase column (100 Å, 5 µm, 300 µm x 50 mm) and an IKey peptide BEH C18 column (130 Å, 1.71 μm, 150 μm x 50 mm). The following gradient was used on the UPLC system: trapping conditions of 97% A and 3% B with a flow rate of 30 µL/min. Initial conditions of 3% B ramping up linearly to 97% B at 5.0 min and held for 1 min. At 7.0 min, the column was stepped down to initial conditions. Mobile phases A and B were H_2O and CH_3CN both containing 0.1% formic acid, respectively. The flow rate was 3.0 µL/min and column temperature was set to 25 ˚C.

Supplemental Results

Isolation of M1 from pooled urine. Given that pH is a valuable tool to change charge states of a molecule and thereby enable various orthogonal separation methods, M1 stability was investigated under acidic, neutral and basic conditions and found to be stable under all conditions for several weeks. As the tertiary nitrogen in steroidal alkaloids is basic, we found that M1 could be retained on strong cation exchange SCX media, but the high salt content of human urine caused early breakthrough. Therefore, 700 mL of urine was loaded on an Omnifit preparative LC-column packed with C18 spherical flash chromatography particles and equilibrated with a 5:95 solution of methanol and water. After loading, the column was rinsed with approximately 10 column volumes of water to remove extremely polar metabolites and salts, and subsequently eluted with a 50:50 mixture of methanol/water resulting in ~100-fold concentration (see Table 1 in parent paper). Fractions were collected during elution and combined based on M1 content. This process was repeated until all 40 L of urine was processed. The volume of the combined fractions was evaporated to ~500 mL, and SCX solid phase extraction (SPE) was conducted to remove non-basic compounds. Fractions of 10 mL were extracted using a batched approach, yielding a total 150 mL of concentrated M1-containing solution. We explored whether strong anion exchange could be used to purify M1, however we were not able to release M1 from the stationary phase in high yield, thus this approach was abandoned. The solution was further purified by preparative chromatography on an analytical scale using a Sunfire C18 column. However, column performance dropped dramatically after only a few injections due to extremely hydrophobic compounds accumulating on the head of the chromatographic bed and irreversibly destroying the column. To address this issue an additional preparative step, analogous to that of step one using flash chromatography, was introduced to remove material that was detrimental for chromatographic columns operating with high efficiency. To purify M1 with high efficiency separation, 150 mL of effluent from the previous step was purified batch-wise on a Sunfire C18 analytical chromatography column with fraction collection. Although M1 was the most abundant molecule in the column effluent, it still was not sufficiently pure for NMR identification. In an attempt to introduce additional selectivity the pH of the mobile phase was changed to pH 10. It was found that M1 was significantly more strongly retained on a BEH C18 chromatographic column than all other interfering compounds that were also present. Small volume injections of M1 solution were purified batch-wise, maximizing the efficiency of the UPLC column to yield pure material by qTOF mass spectrometry and subsequently subjected to NMR analysis for structural elucidation.

Equation S1. Number of double bond equivalents.

$$DBE = C - \frac{H}{2} + \frac{N}{2} + 1$$

Figure S1. Enhanced view of ^{1}H NMR spectrum of the solanidine showing four methyl resonances in CD_3OD. Insert showing C6-H (δ = 5.45, $^{3}J_{H\text{-}H}$ = 5.6 Hz, 1H) and C3-H (δ = 3.40, m, 1H) resonances.

Figure S2. ^{1}H spectrum of SSDA.

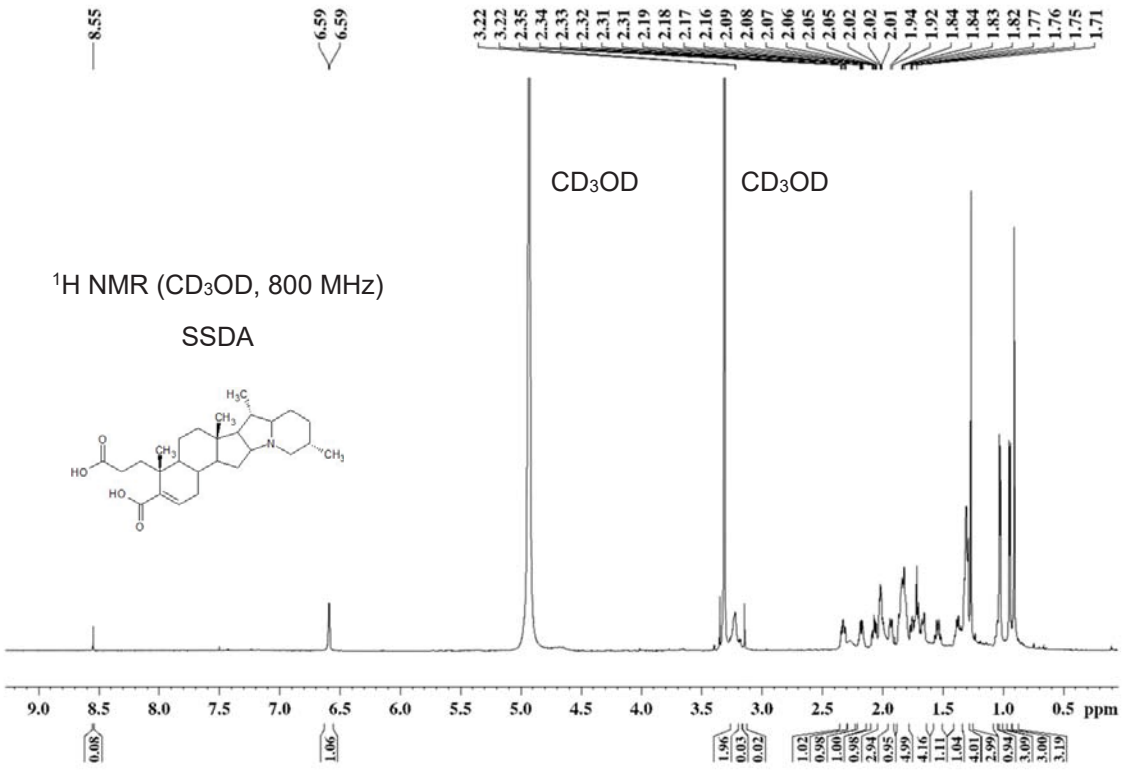

Figure S3. Enhanced view of ^{1}H NMR spectrum of the unknown CYP2D6 biomarker showing four methyl resonances in CD_3OD. Insert showing methylylidene resonance.

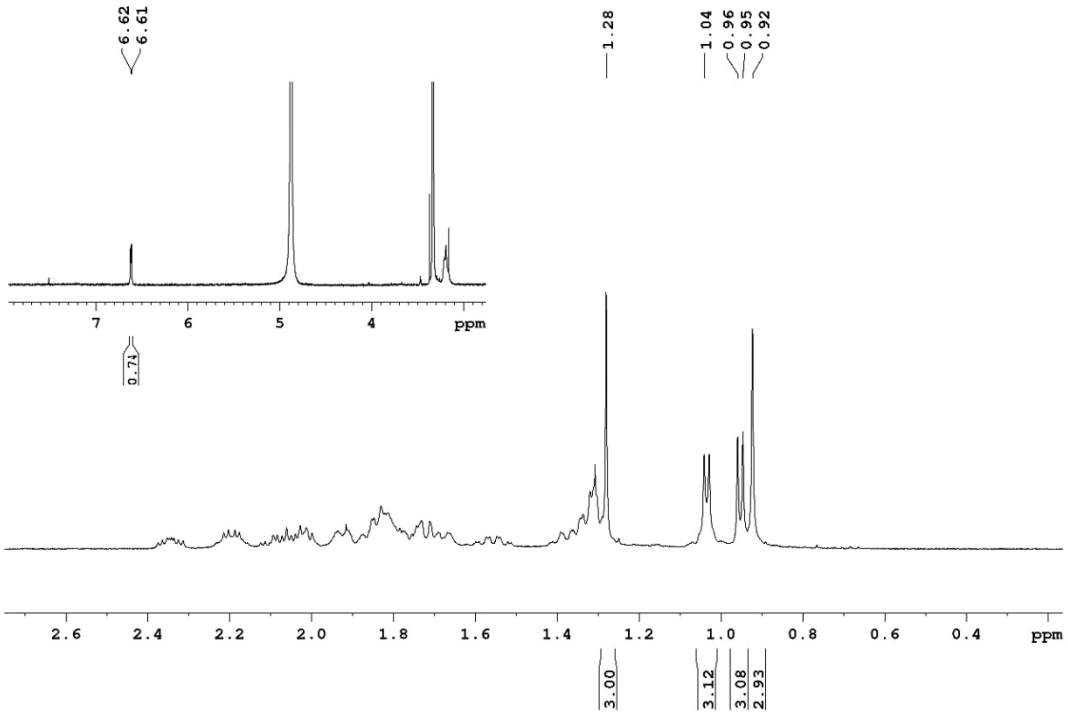

Figure S4. Stepwise connectivity model of unknown CYP2D6 biomarker. a = Ambiguous assignment of C-1, C-2 and C-24. X = C or heteroatom. Hydrogen atoms omitted for clarity.

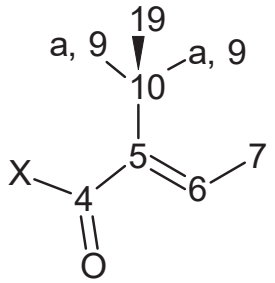

Figure S5. Stepwise connectivity model of unknown CYP2D6 biomarker. a = Ambiguous assignment of carbons 1, 2, 24. X = C or heteroatom. Hydrogen atoms omitted for clarity.

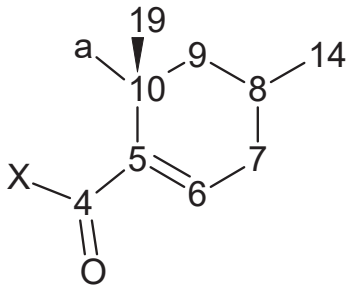

Figure S6. 2D TOCSY with enhanced view of C2-H' correlations with C1-H' and/or C15-H'. Red circle represents missing C15-H correlation.

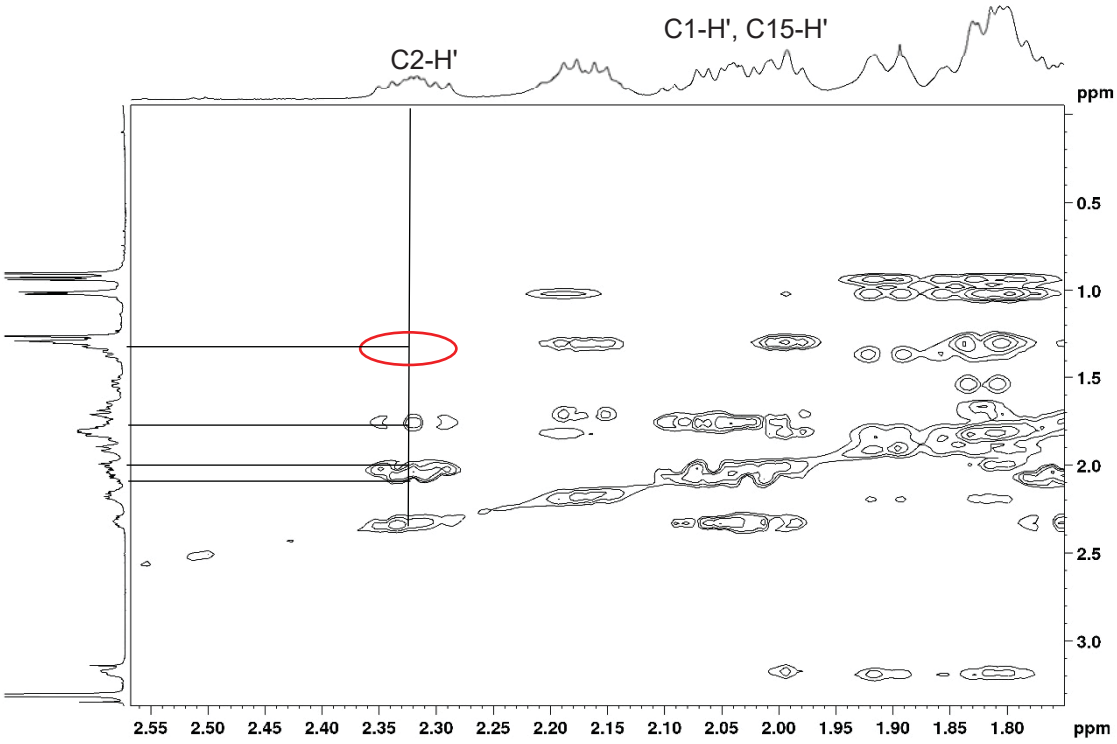

Figure S7. 2D TOCSY with enhanced view of C1-H' and C1-H correlations C2-H' and C2-H.

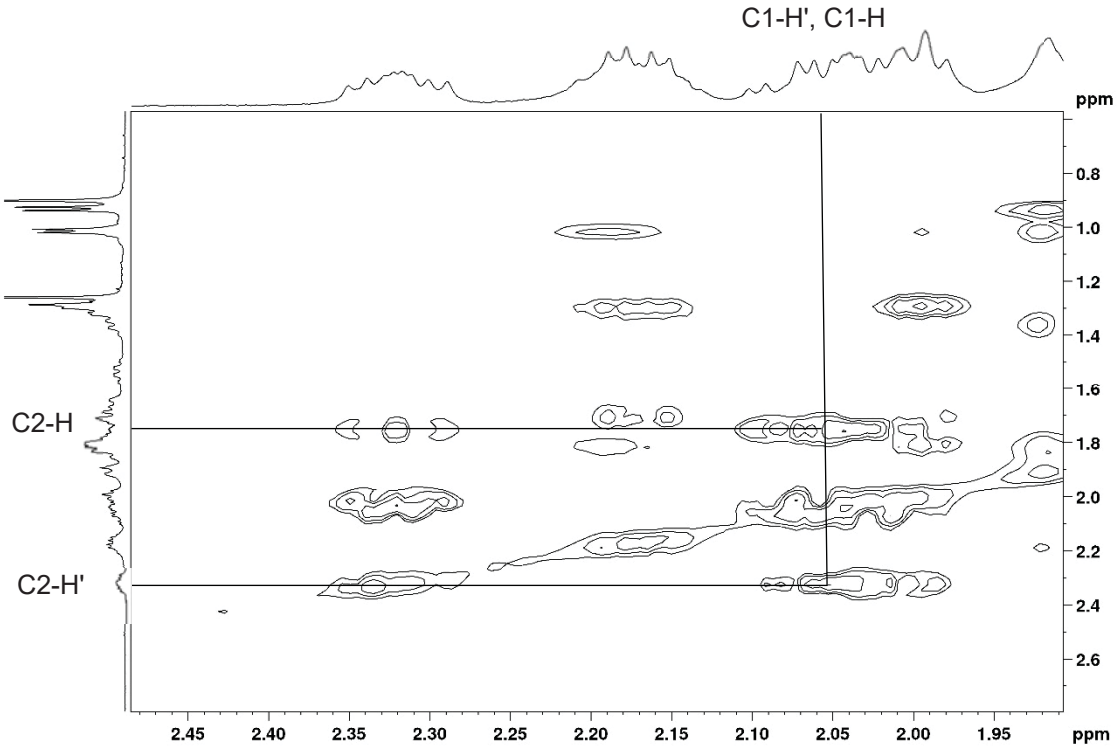

Figure S8. Stepwise connectivity model of unknown CYP2D6 biomarker. X = C or heteroatom. Hydrogen atoms omitted for clarity.

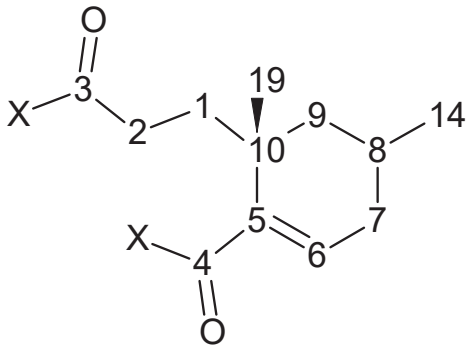

Figure S9. Stepwise connectivity model of unknown CYP2D6 biomarker. X = C or heteroatom. Hydrogen atoms omitted for clarity.

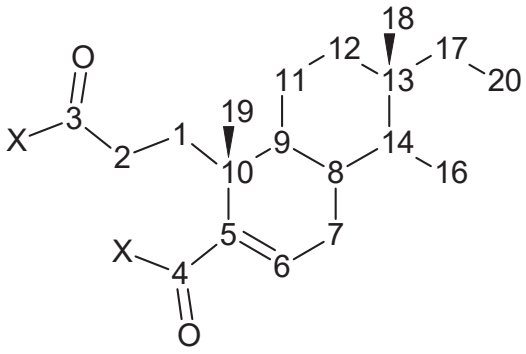

Figure S10. Stepwise connectivity model of unknown CYP2D6 biomarker. X = C or heteroatom; R = C or heteroatom; R' = C or heteroatom. Hydrogen atoms omitted for clarity.

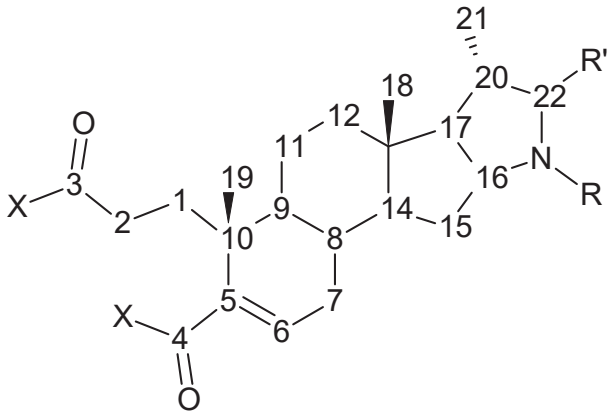

Figure S11. Stepwise connectivity model of unknown CYP2D6 biomarker. X = heteroatom. Hydrogen atoms omitted for clarity.

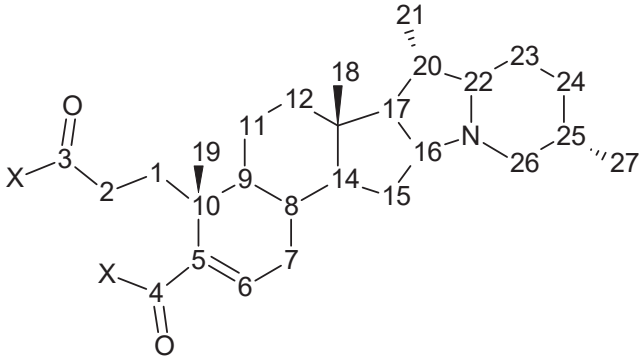

Figure S12. $^{13}C\{^{1}H\}$ NMR spectrum of SSDA.

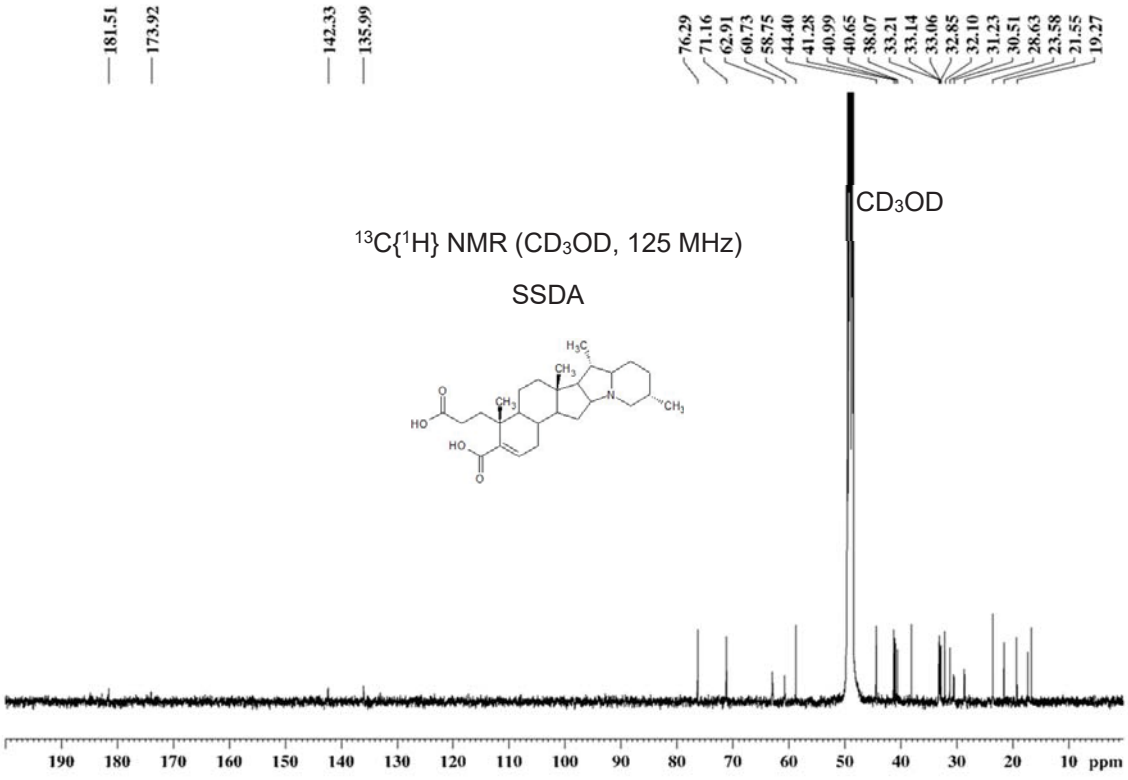

Figure S13. Enhanced $^{13}C\{^{1}H\}$ NMR spectrum of SSDA.

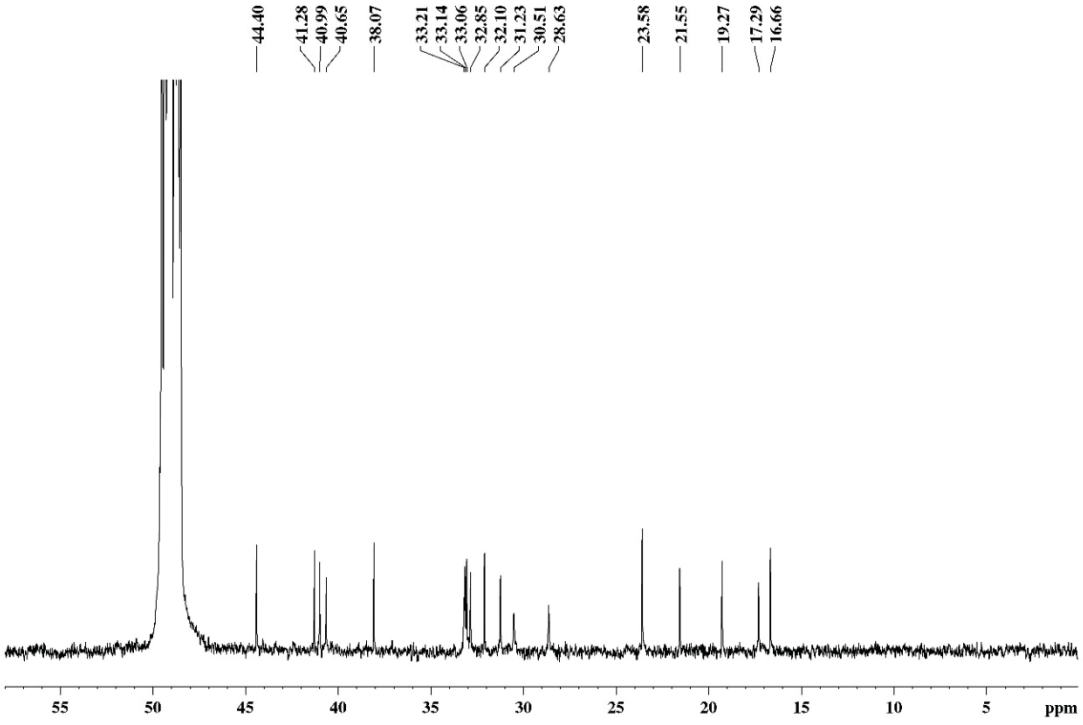

Figure S14. DEPT135 $^{13}C\{^{1}H\}$ NMR spectrum of SSDA.

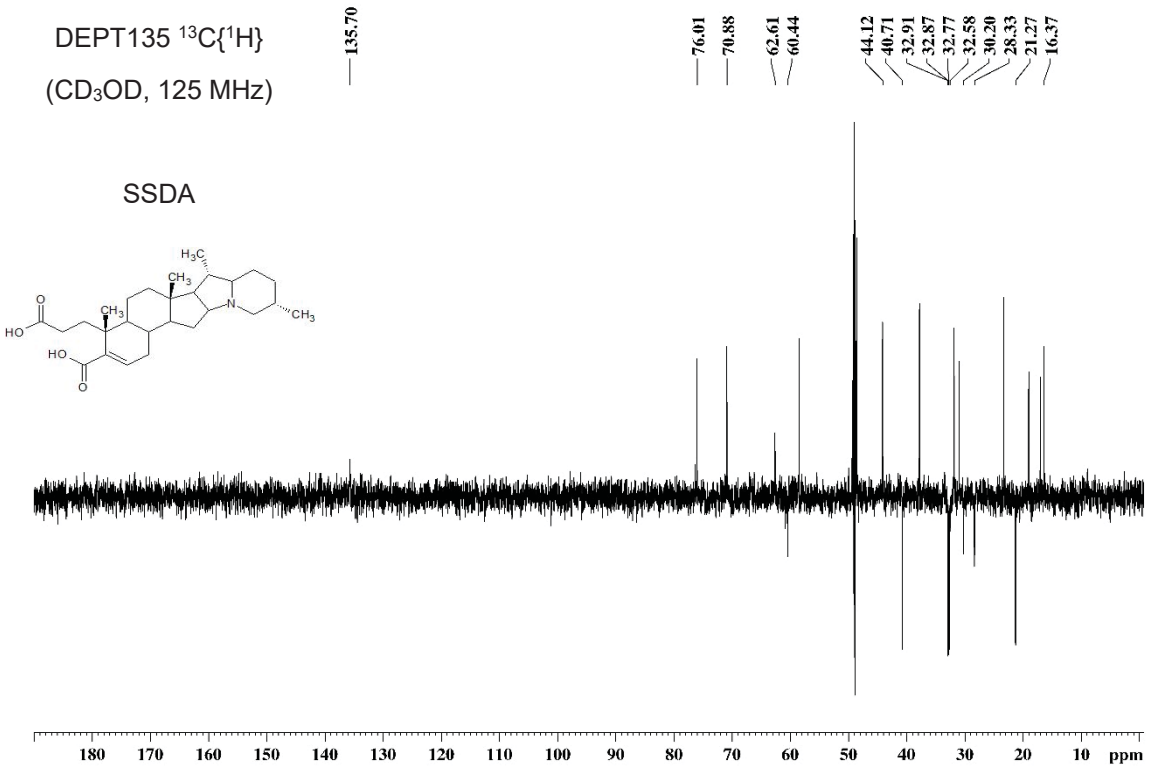

Figure S15. DEPT90 $^{13}C\{^{1}H\}$ NMR spectrum SSDA.

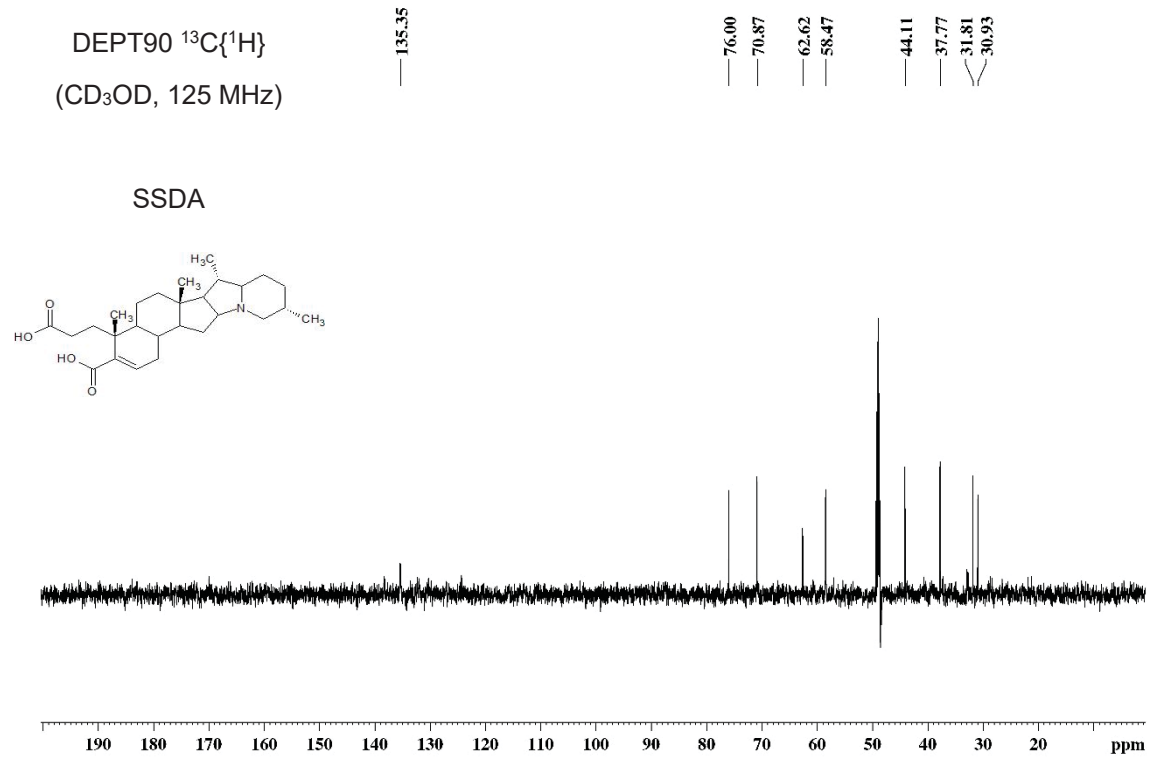

Figure S16. HSQC full spectrum of SSDA in CD_3OD.

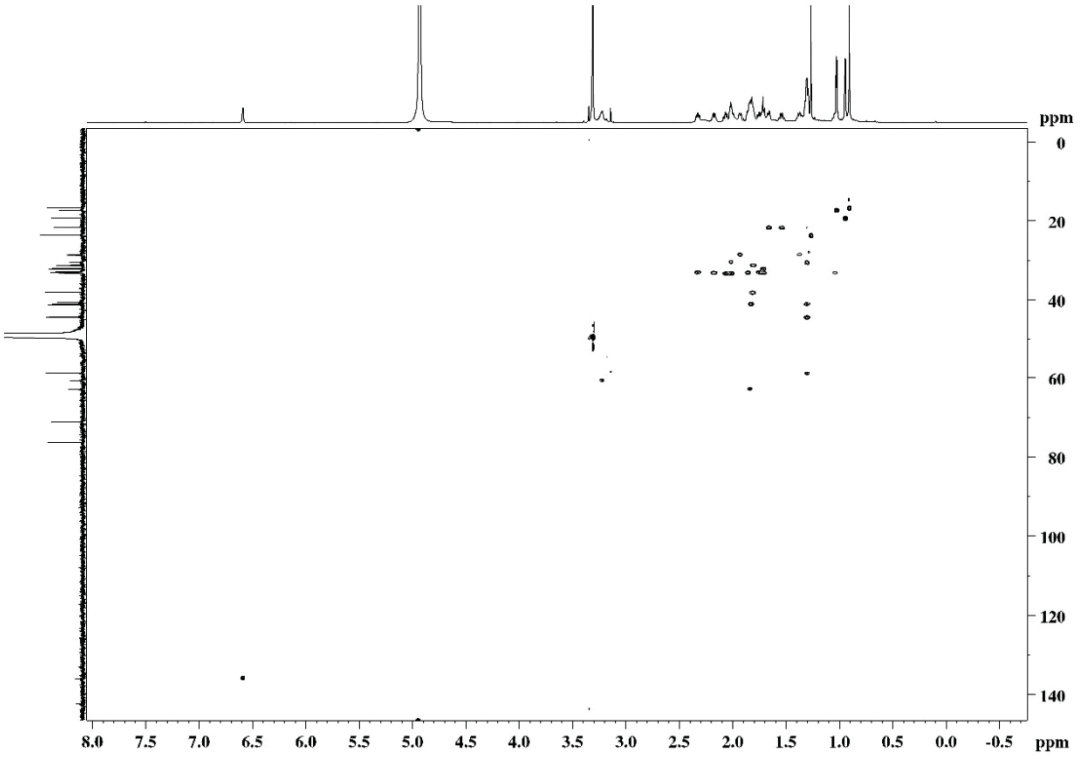

Figure S17. HSQC enhanced spectrum of SSDA in CD_3OD.

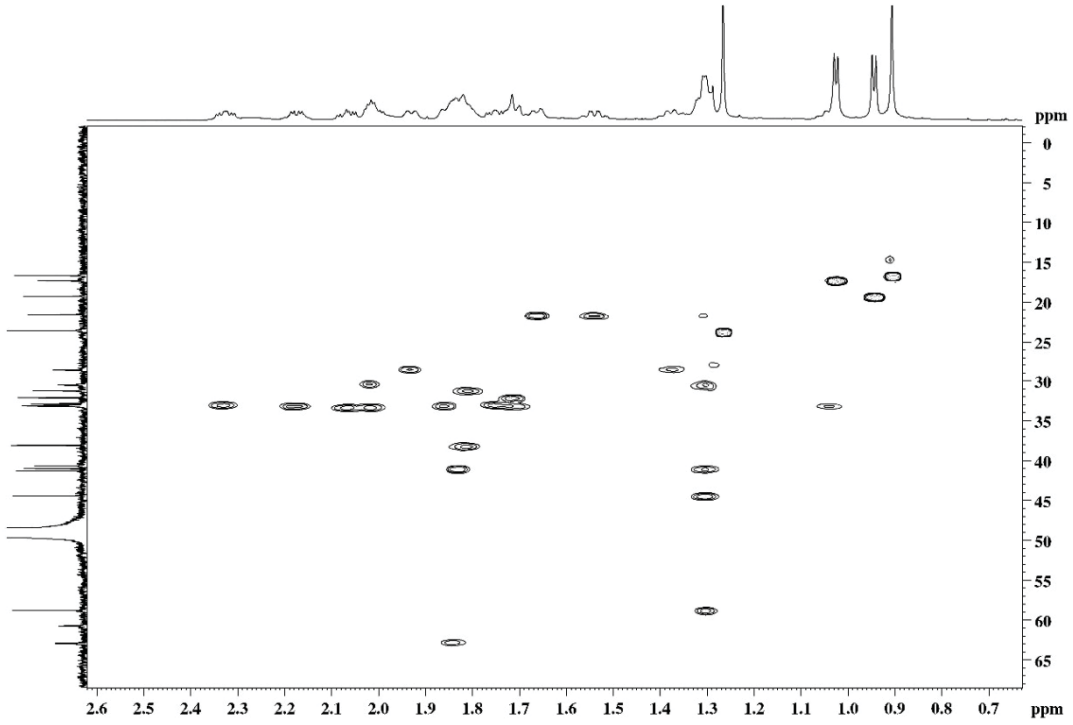

Figure S18. HMBC spectrum of SSDA in CD_3OD.

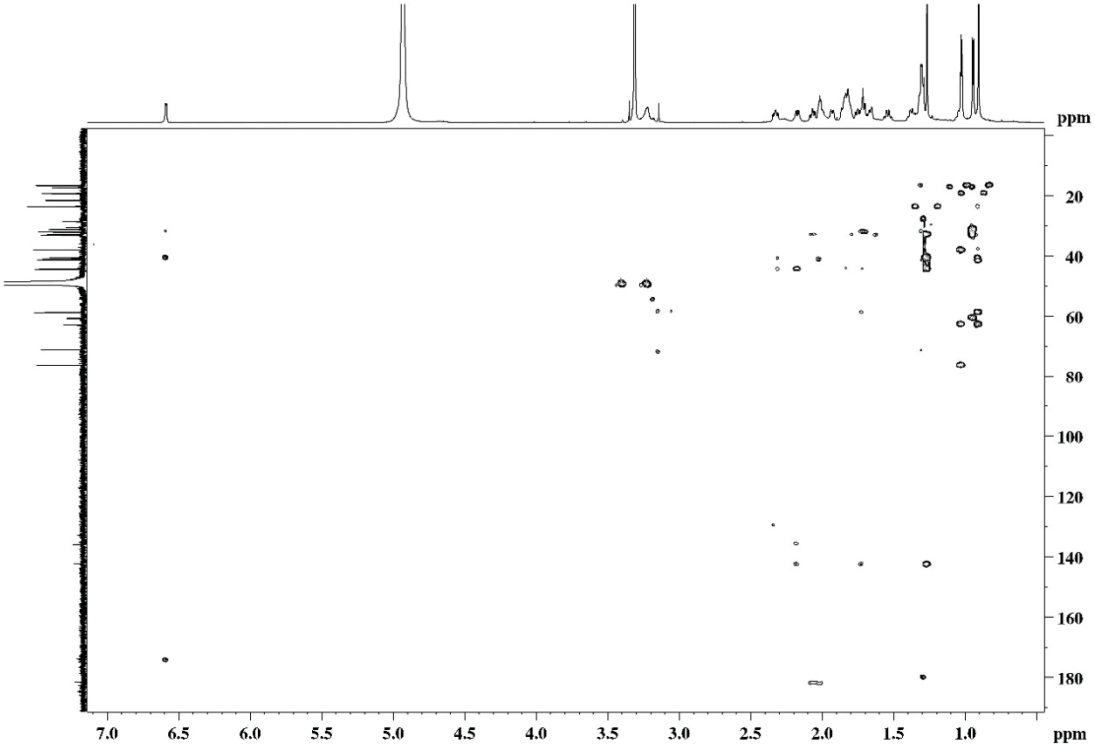

.**Figure S19.** HMBC spectrum of SSDA in CD_3OD with C6−H correlations.

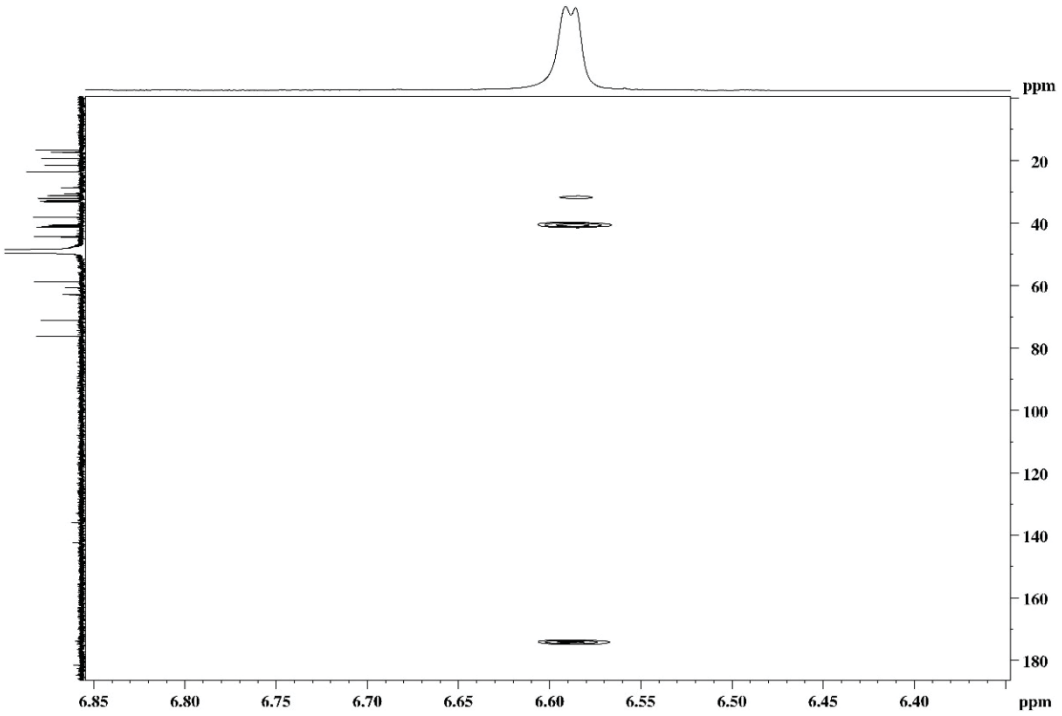

Figure S20. HMBC enhanced spectrum of SSDA in CD_3OD.

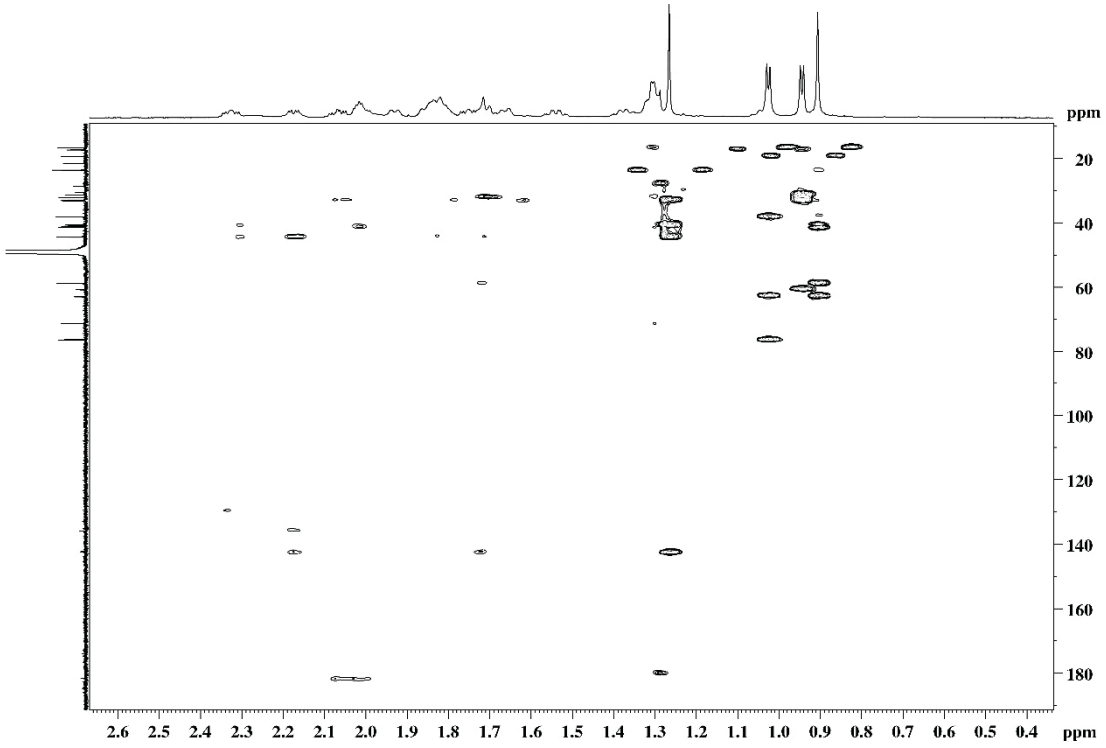

Figure S21. HMBC enhanced spectrum of SSDA in CD_3OD with C18−H, C19−H, C21−H and C27−H correlations.

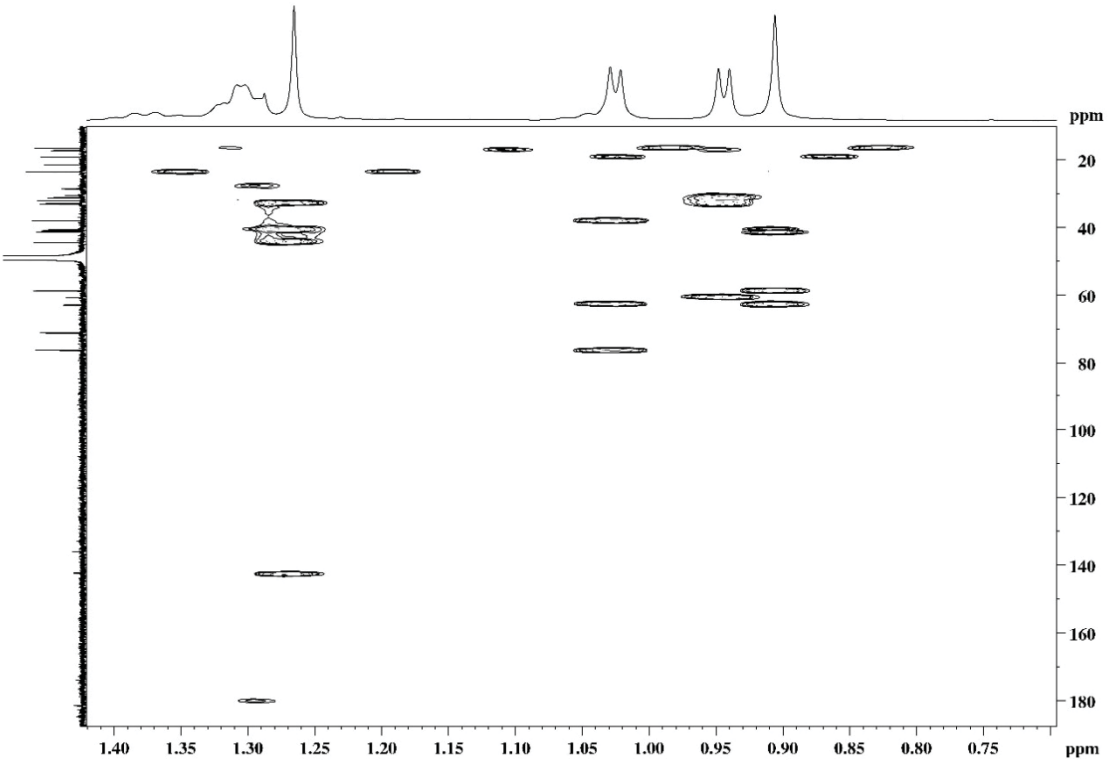

Figure S22. HMBC spectrum of SSDA in CD_3OD with long range J filter width = 6 Hz.

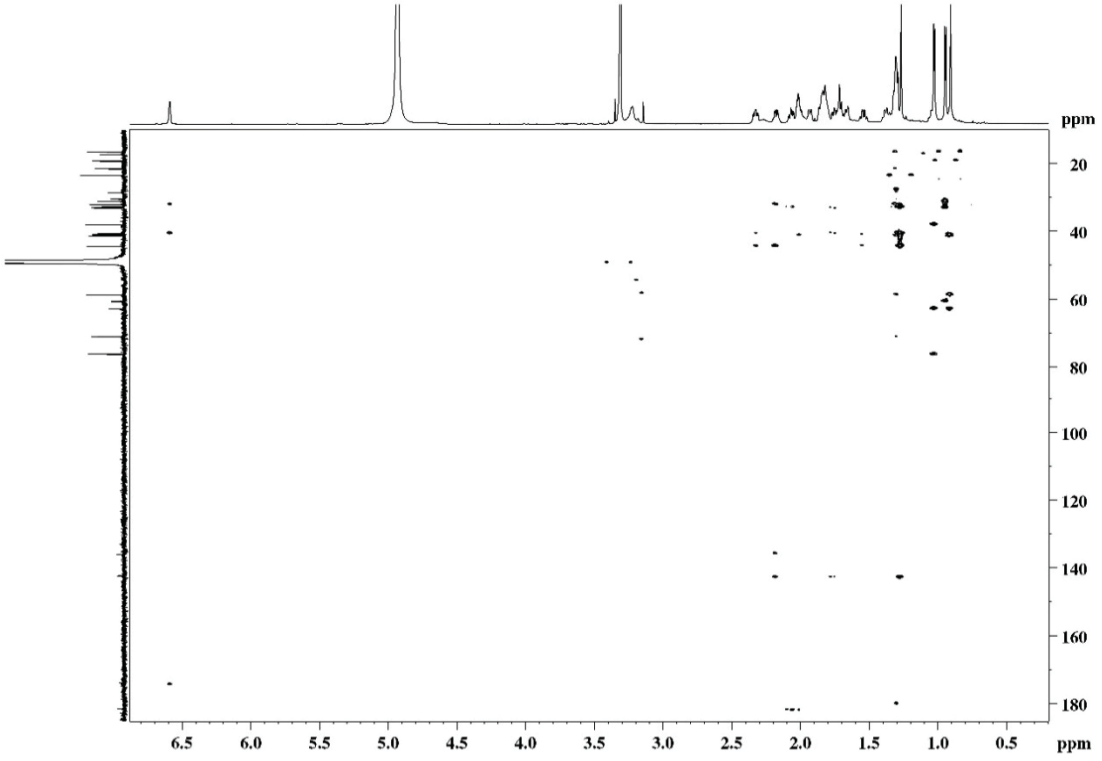

Figure S23. HMBC enhanced spectrum of SSDA in CD_3OD with long range J filter width = 6 Hz.

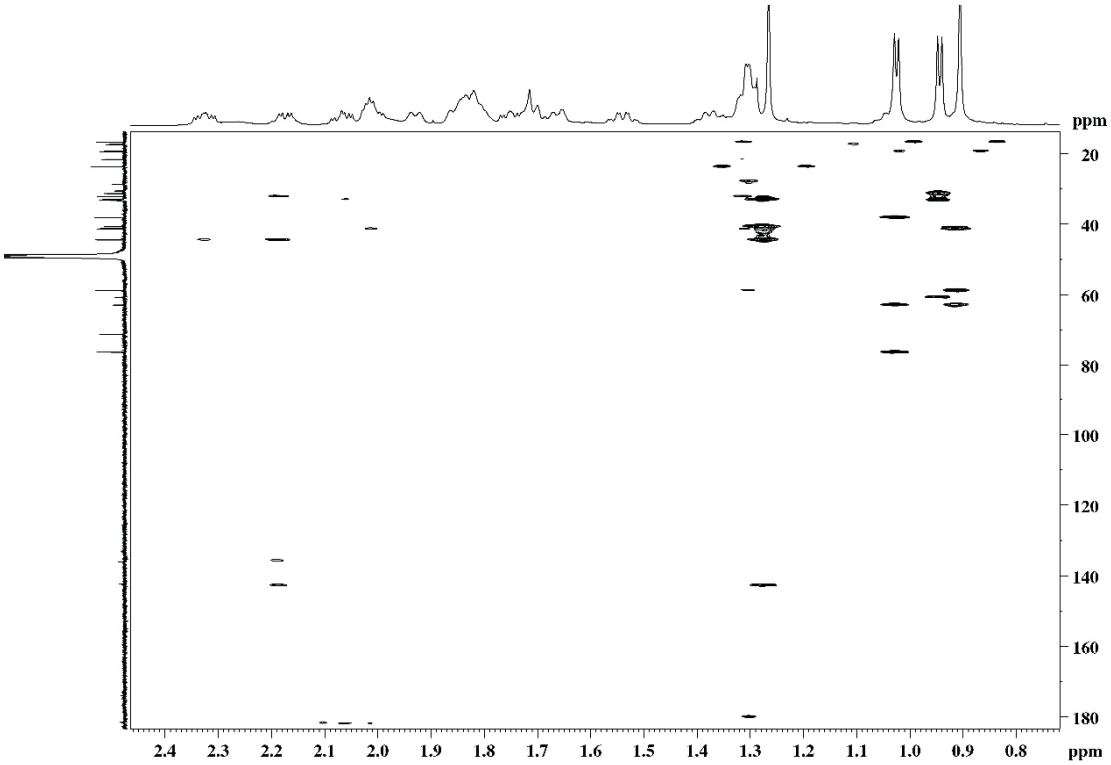

Figure S24. HMBC spectrum of SSDA in CD_3OD with long range J filter width = 4 Hz.

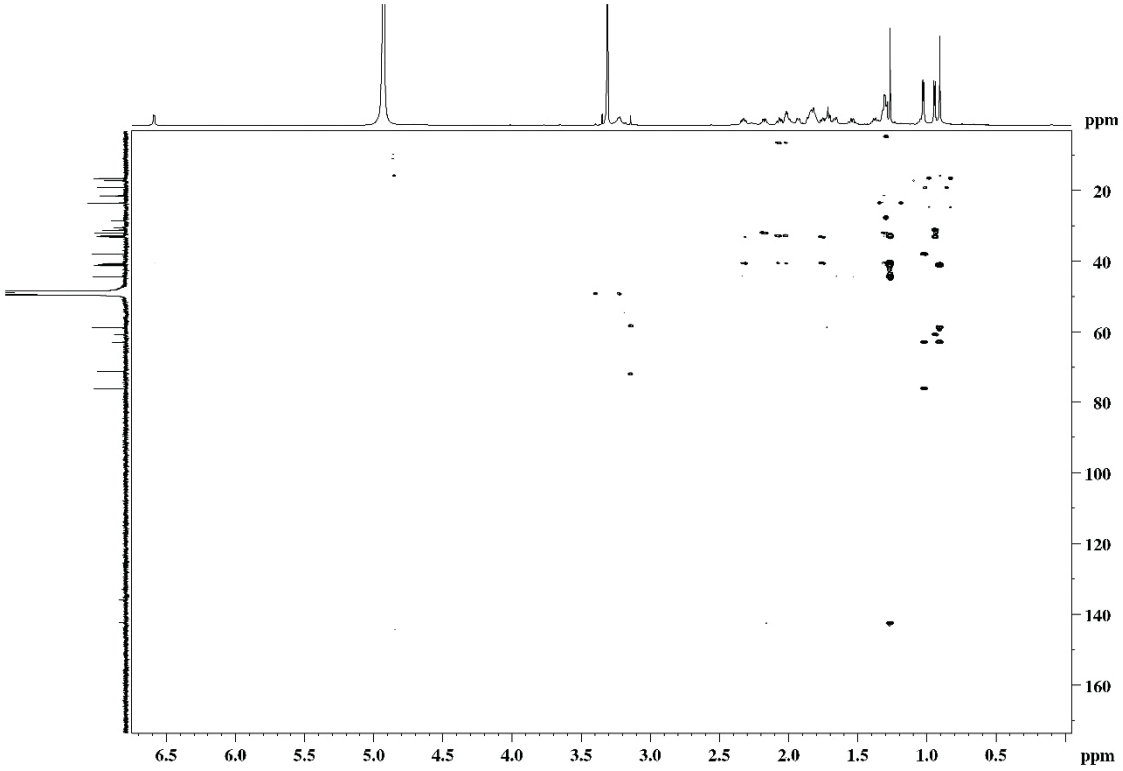

Figure S25. HMBC enhanced spectrum of SSDA in CD_3OD with long range J filter width = 4 Hz.

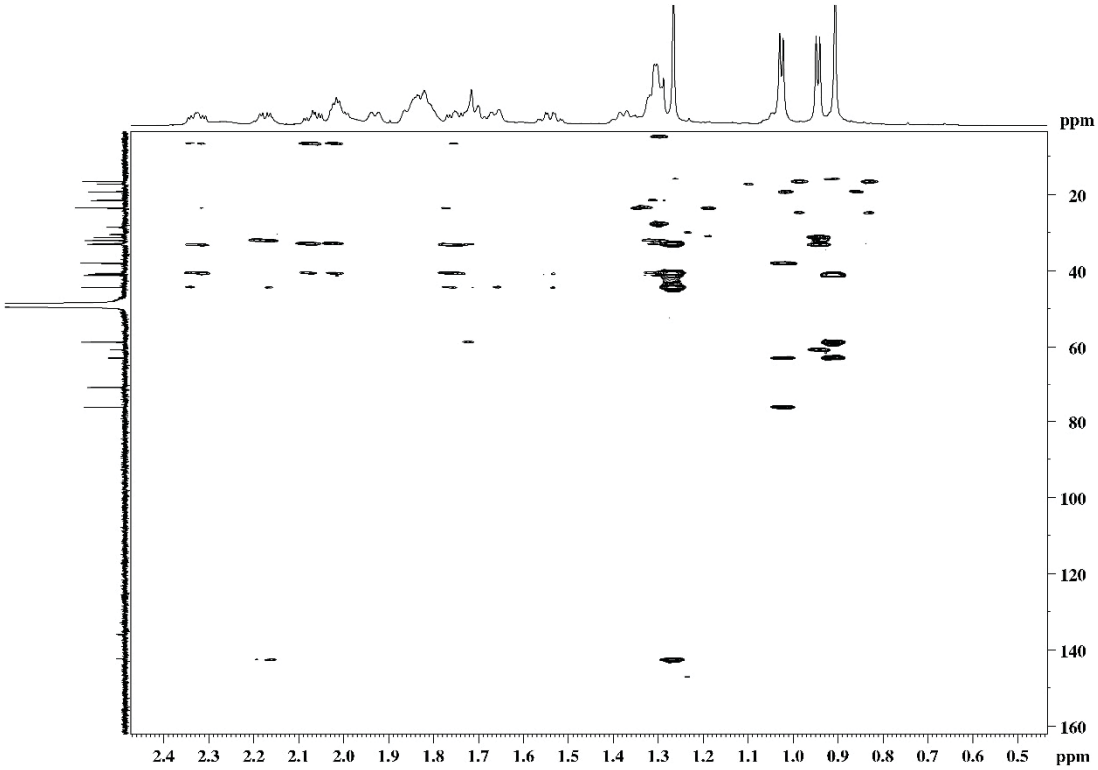

Figure S26. COSY spectrum of SSDA in CD_3OD.

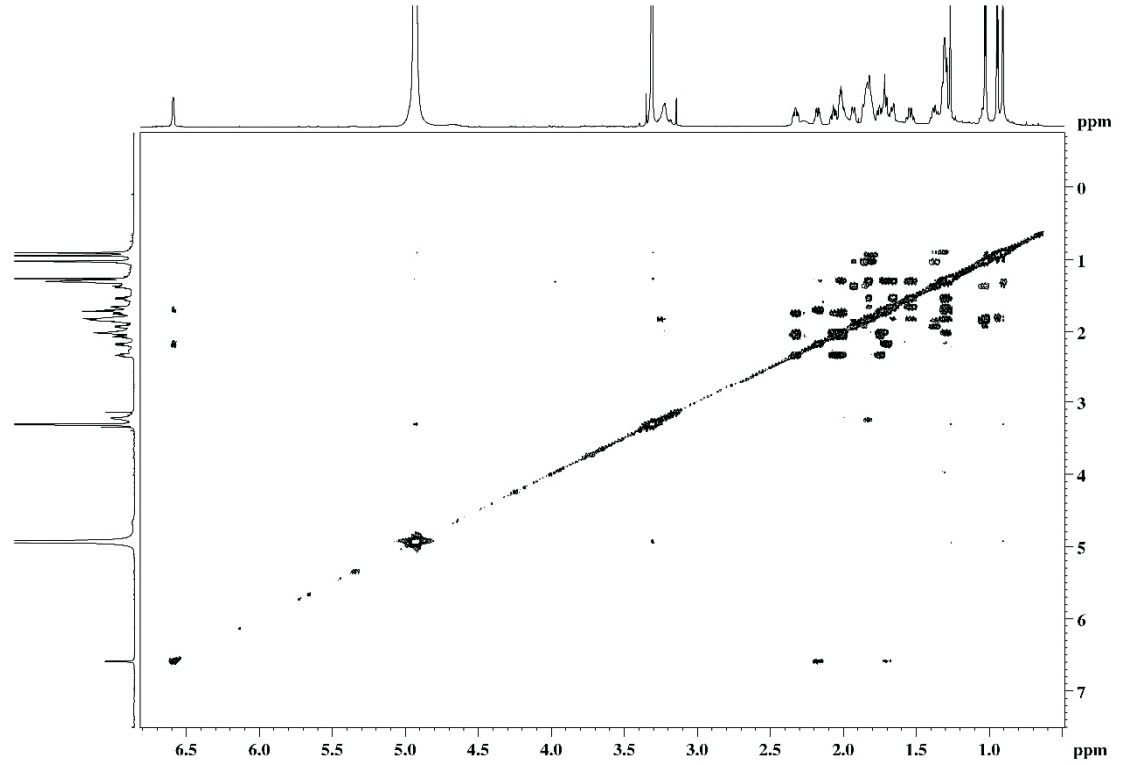

Figure S27. COSY enhanced spectrum of SSDA in CD_3OD with C6−H correlations.

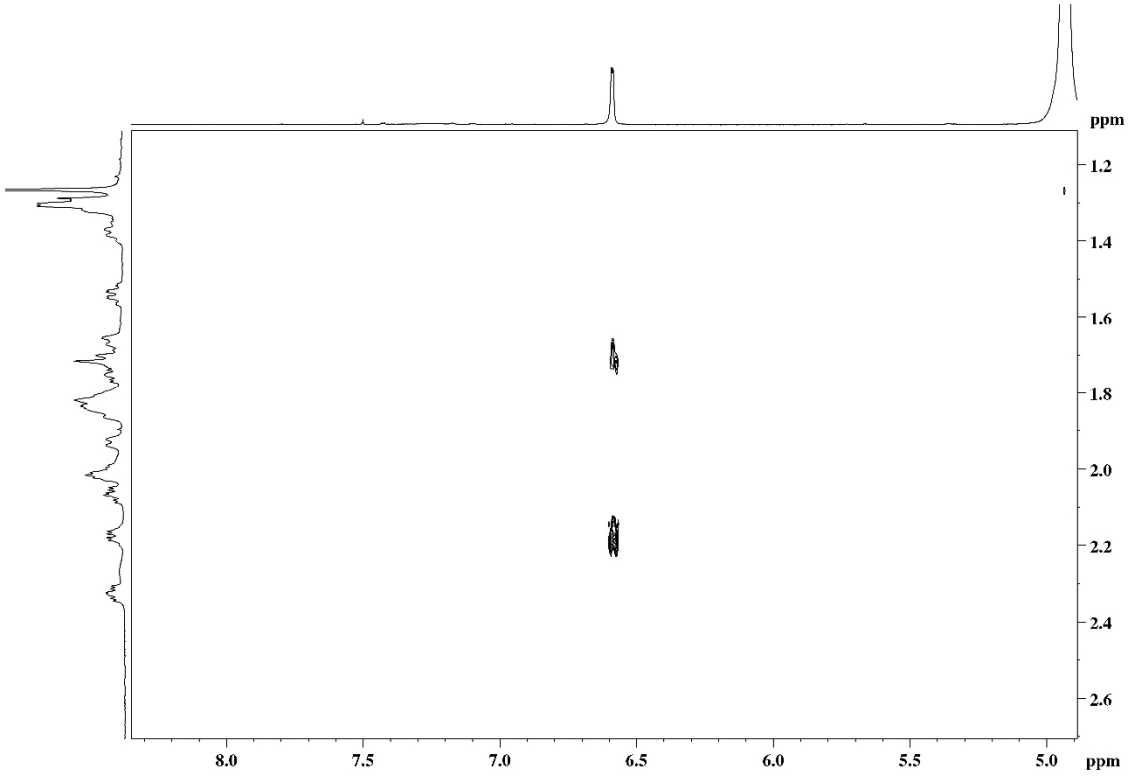

Figure S28. COSY enhanced spectrum of SSDA in CD_3OD.

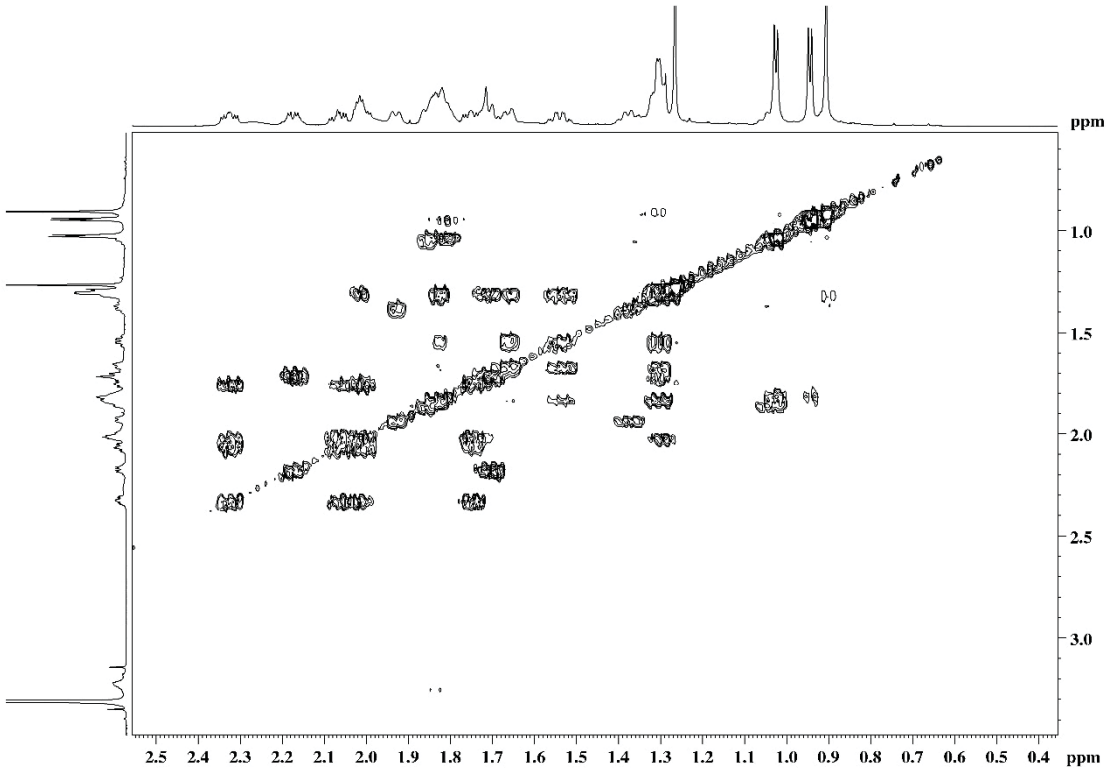

Figure S29. TOCSY spectrum of SSDA in CD_3OD.

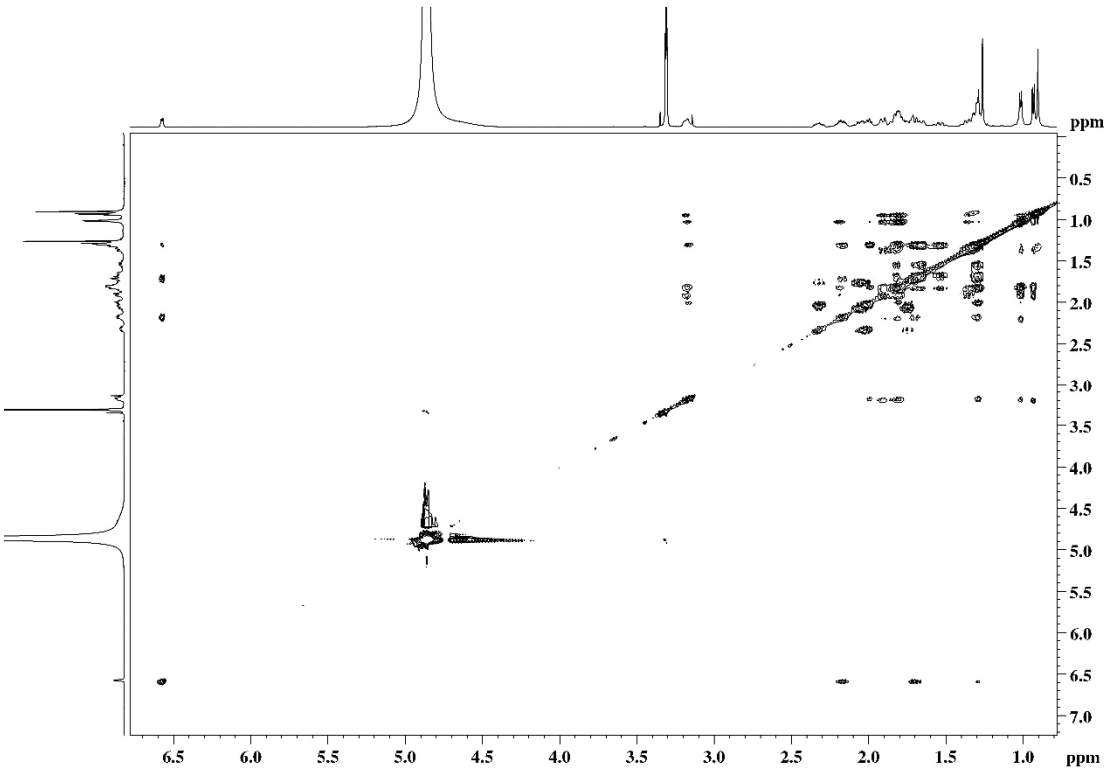

Figure S30. TOCSY enhanced spectrum of SSDA in CD_3OD with C6−H correlations.

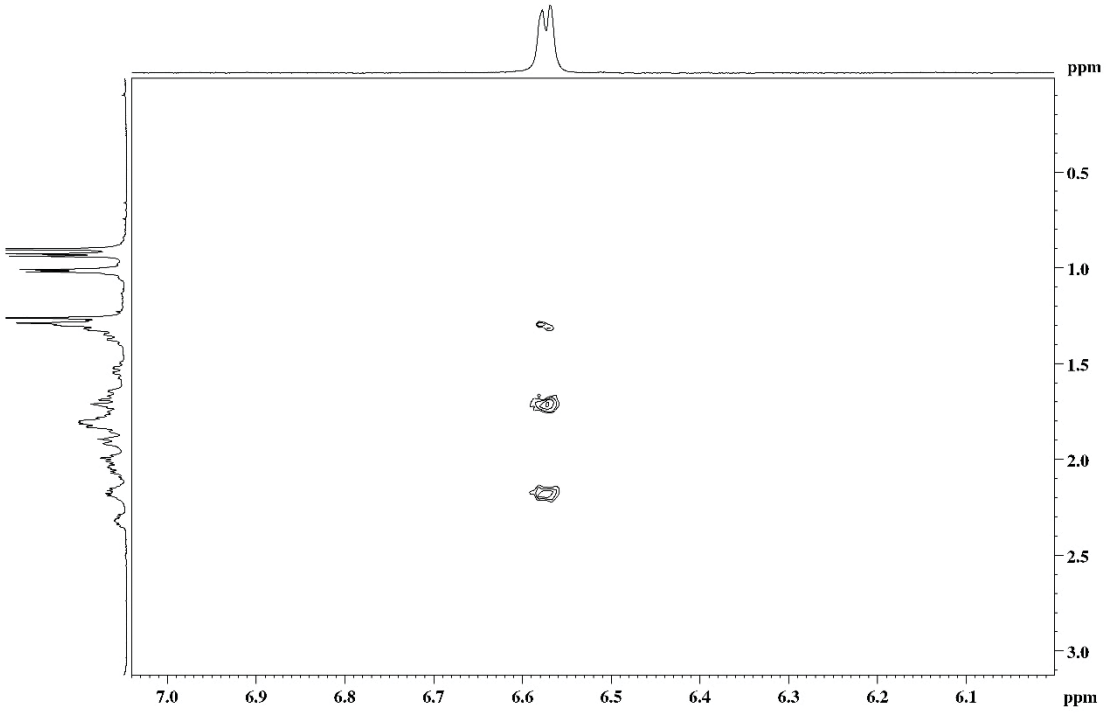

Figure S31. TOCSY enhanced spectrum of SSDA in CD_3OD.

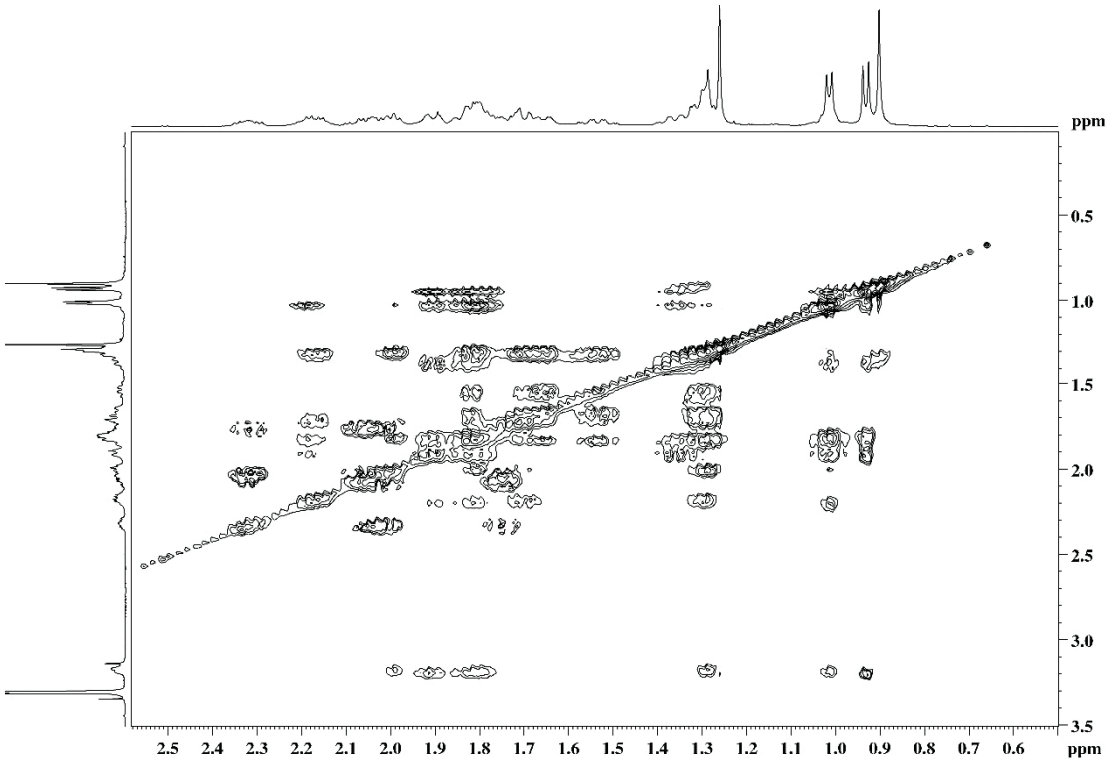

Figure S32. TOCSY enhanced spectrum of SSDA with view of C15-H correlations. Red circle represents missing correlation.

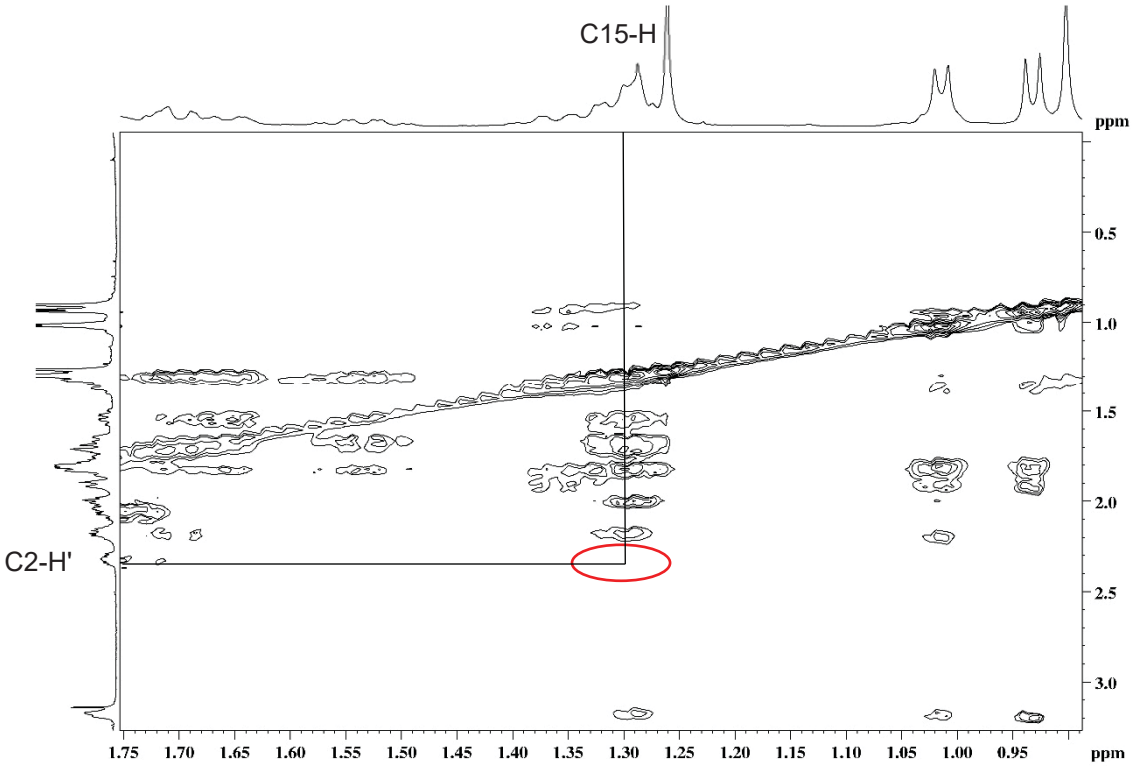

Figure S33. HSQC−TOCSY enhanced spectrum of SSDA in CD_3OD.

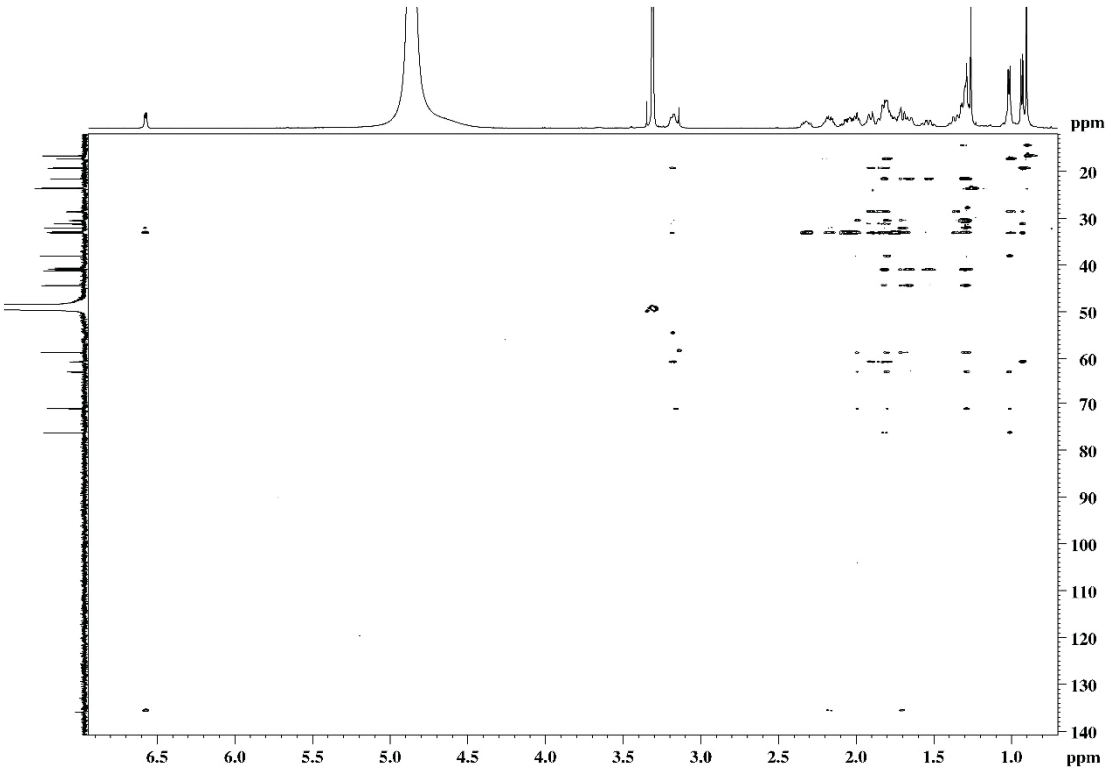

Figure S34. HSQC−TOCSY enhanced spectrum of SSDA in CD_3OD with C6−H correlations.

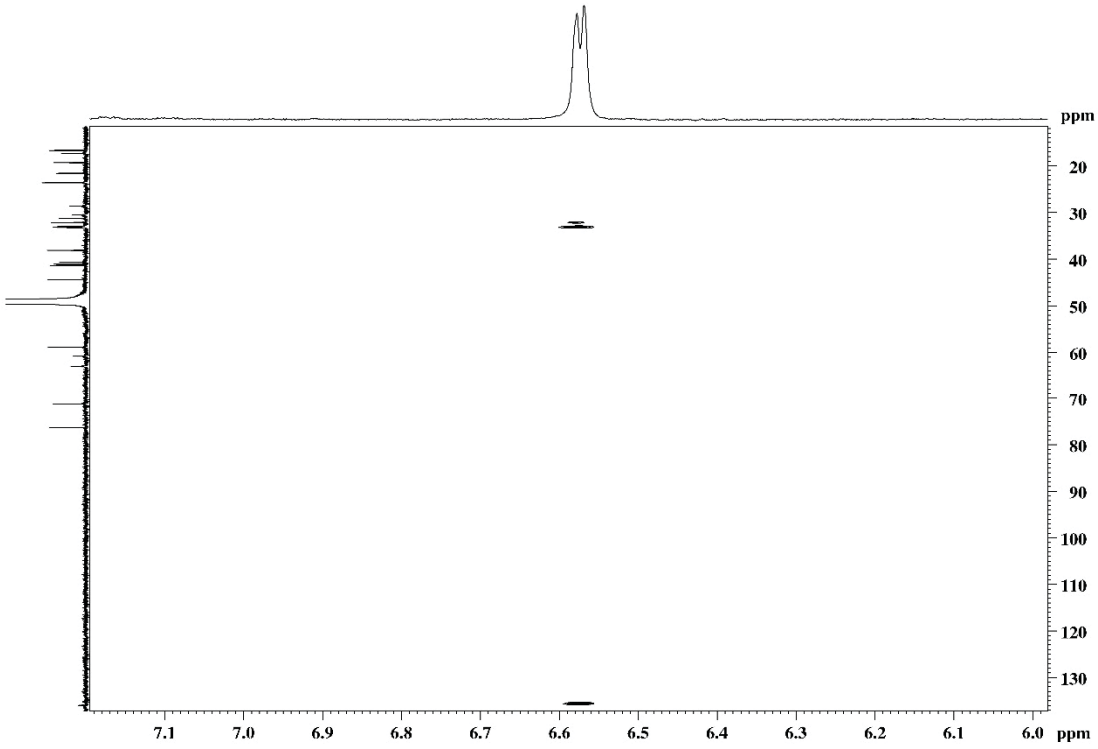

Figure S35. HSQC−TOCSY enhanced spectrum of SSDA in CD_3OD.

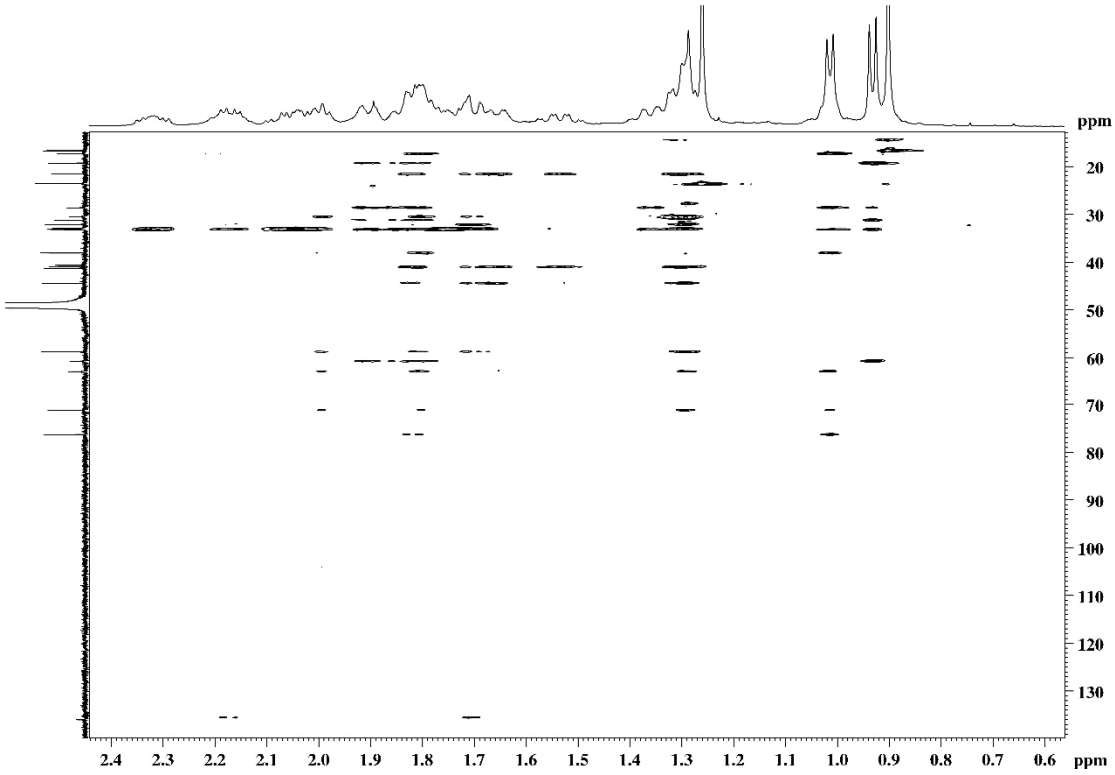

Figure S36. HSQC−TOCSY enhanced spectrum of SSDA in CD_3OD with spectral window 2.5−1.5 ppm.

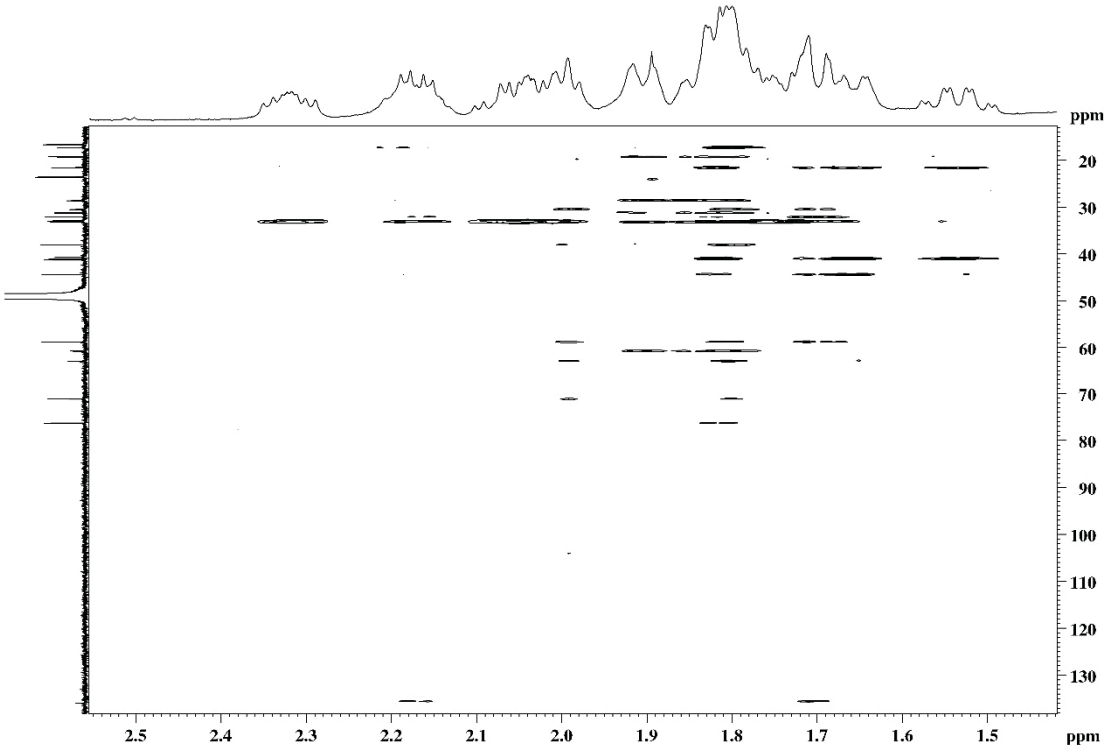

Figure S37. HSQC−TOCSY enhanced spectrum of SSDA in CD_3OD with C21−H and C27−H correlations.

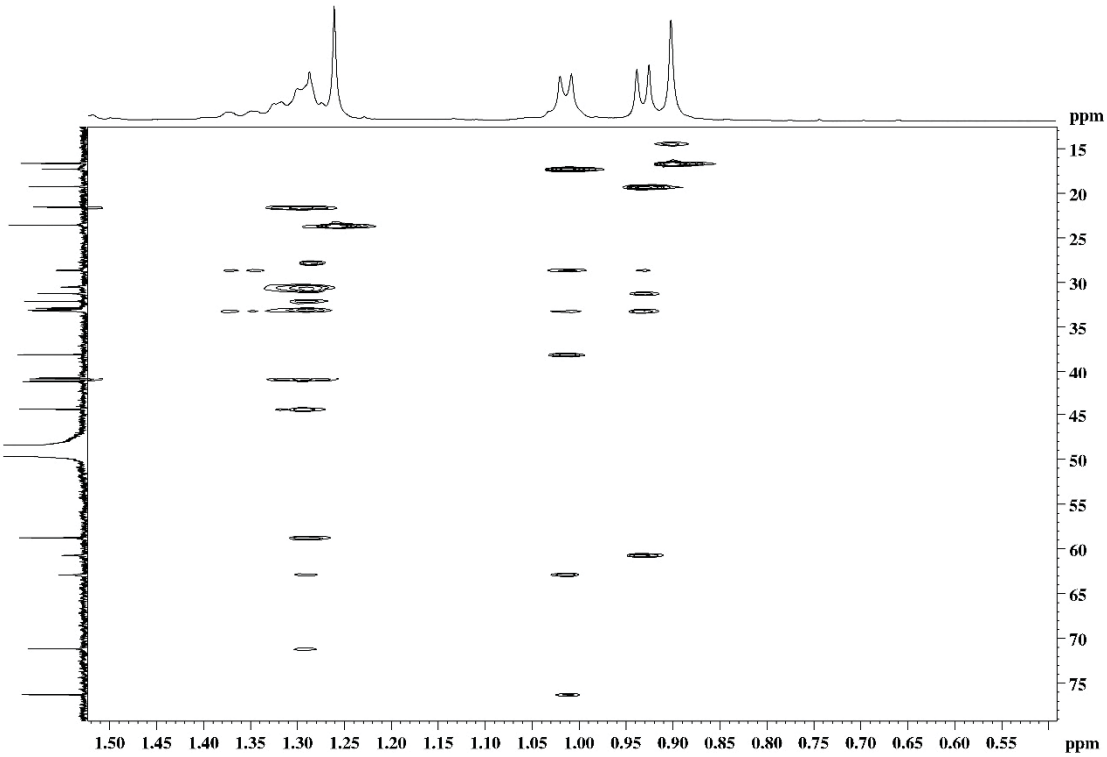

Figure S38. Amidation of SSDA with EDC and ethanolamine and chromatogram of first amidation product of SSDA.

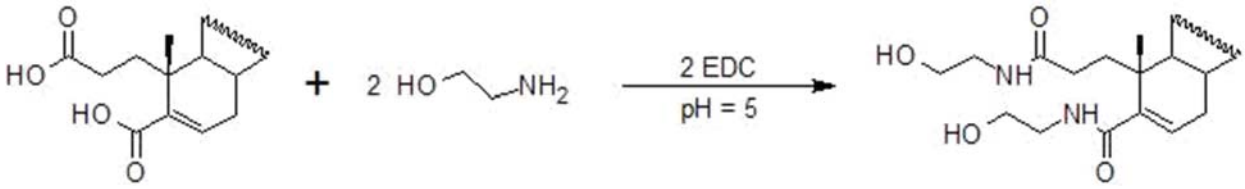

Figure S39. Chromatogram of second amidation product of SSDA.

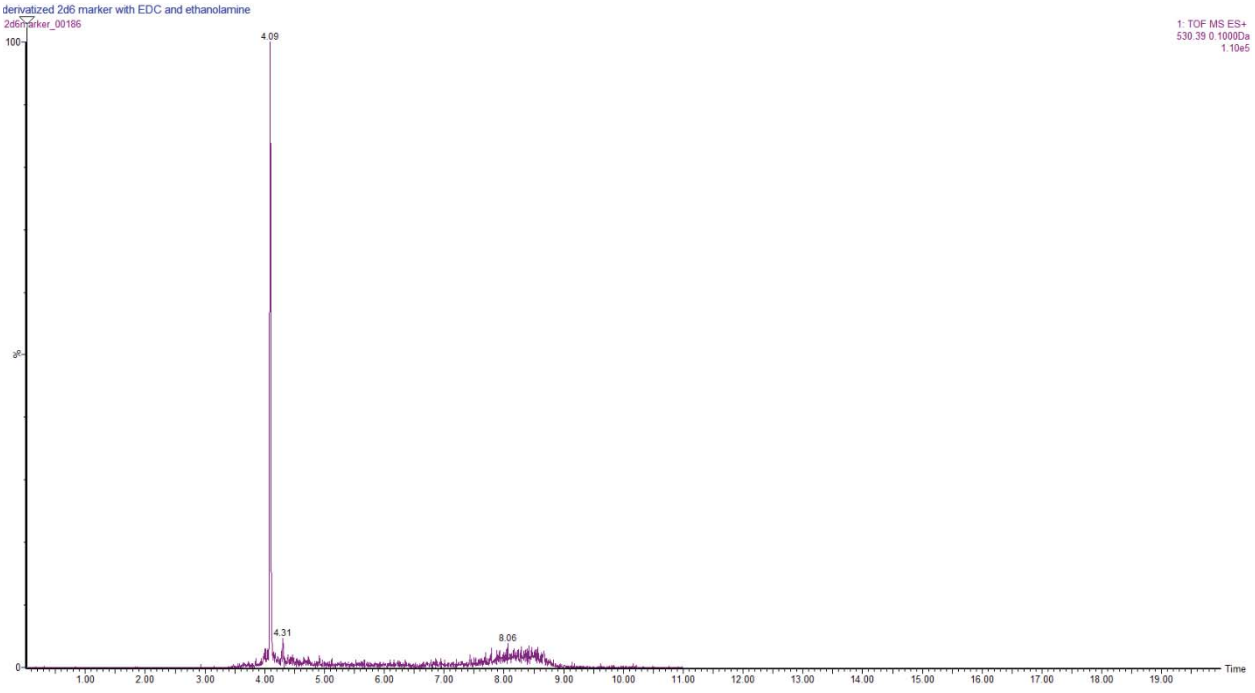

Table S1. qNMR Results

analyte	δ	number of protons (n)	Integral (Int)	Concentration of SSDA	Moles of SSDA	Amount of SSDA (μg)
IC	8.50000000	2.00000000	2.00000000	0.00044152	0.00000022297	98.81
IC	7.75000000	1.00000000	1.04470000	0.00042262	0.00000021343	94.68
IC	7.40000000	2.00000000	2.11480000	0.00041755	0.00000021086	93.54
SSDA	6.60000000	1.00000000	0.90160000			

IC = internal standard = pyridine, anhydrous, 99.8%

[IC] = internal standard concentration in NMR tube = 0.00048970 mol/L

Total volume of NMR sample = 505 µL

MW_{SSDA} = molecular weight of SSDA = 443.6187 g/mol

n_{IC} = number of protons that give rise to signal of internal calibrant

n_{SSDA} = number of protons that give rise to signal of SSDA

Int_{IC} = integral value of internal calibrant

Int_{SSDA} = integral value of SSDA

Sample calculation of concentration of SSDA = $[pyridine]*[Int_{SSDA}/Int_{IC}]*[n_{IC}/n_{SSDA}]$ = 0.00044152 moles/L

Moles of SSDA = [SSDA]*[volume of solution] = 0.223 µmoles

Grams of SSDA = $[moles\ of\ SSDA]*[MW_{SSDA}]$ = 98.81 µgrams

Table S2. qNMR Results and step-by-step Workflow 100% Method to Determine Purity

analyte	δ	number of protons	integral	normalized integral (nInt)
SSDA	6.60000000	1.00000000	0.90160000	90.1600

	δ	number of protons	integral	normalized integral (nInt)
pyridine	8.50000000	2.00000000	2.00000000	100.0000
	7.75000000	1.00000000	1.04470000	104.4700
	7.40000000	2.00000000	2.11480000	105.7400

Equations taken from (Pauli et al. 2014)

MW_{SSDA} = molecular weight of SSDA = 443.6187 g/mol

$MW_{pyridine}$ = molecular weight of internal calibrant = 79.10 g/mol

$nInt_{SSDA}$ = normalized integral for SSDA signal (integral value normalized to value of number of protons) = 90.16/1 = 90.16

$nInt_{pyridine}$ = normalized integral for pyridine signal (integral value normalized to value of number of protons)

$\Sigma(nInt_{pyridine})$ = [(200.00/2 + 104.47/1 + 211.48/2)/5] = 62.04

Purity = P [%] = $\frac{nInt_{SSDA} * MW_{SSDA}}{nInt_{SSDA} * MW_{SSDA} + \sum(nInt_{pyridine} * MW_{pyridine})} * 100$ = 99.85%

Table S3. qNMR Results and step-by-step Workflow IC Method to Determine Purity

Chemical shift (δ)	**n** (number of protons)	**Int** (intergral value)	Concentration of SSDA [M]	Moles of SSDA	Amount of SSDA (*u*g)	Purity (%) of SSDA
8.54	2	2.0000	0.0004415	0.0000002230	98.91	99.8
7.85	1	1.0447	0.0004226	0.0000002134	94.68	99.8
7.44	2	2.1148	0.0004176	0.0000002109	93.54	99.8
6.56	1	0.9016				

Equations taken from (Pauli et al. 2014)

Internal calibrant = pyridine (concentration = 0.0004897 M)

Volume of solution (µL) = 505.00

mol_{IC} = moles of internal calibrant

mol_{SSDA} = moles of SSDA

m_{IC} = mass of internal calibrant sample

m_{SSDA} = mass of SSDA sample

P_{IC} = purity of internal calibrant = 99.8%

n_{IC} = number of protons that give rise to signal of internal calibrant

n_{SSDA} = number of protons that give rise to signal of SSDA

Int_{IC} = integral value of internal calibrant

Int_{SSDA} = integral value of SSDA

MW_{IC} = molecular weight of internal calibrant = 79.10 g/mol

MW_{SSDA} = molecular weight of SSDA = 443.6187 g/mol

Molar ratio by intergrals = $\frac{mol_{IC}}{mol_{SSDA}} = \frac{\frac{Int_{IC}}{n_{IC}}}{\frac{Int_{SSDA}}{n_{SSDA}}} = \frac{Int_{IC} * n_{SSDA}}{n_{IC} * Int_{SSDA}}$

Purity = P [%] = $\frac{n_{IC} * Int_{SSDA} * MW_{SSDA} * m_{IC}}{n_{SSDA} * Int_{IC} * MW_{IC} * m_{SSDA}} * P_{IC}$ = 99.8 %

Reference

Pauli GF, Chen S-N, Simmler C, Lankin DC, Gödecke T, Jaki BU, Friesen JB, McAlpine JB, Napolitano JG (2014). Importance of purity evaluation and the potential of quantitative 1H NMR as a purity assay. *J Med Chem* **57**:9220-9231.